Systematic Entomology

Systematic Entomology (2017), **42**, 575–595

Millipede assassins and allies (Heteroptera: Reduviidae: Ectrichodiinae, Tribelocephalinae): total evidence phylogeny, revised classification and evolution of sexual dimorphism

MICHAEL FORTHMAN[1,2] and CHRISTIANE WEIRAUCH[1]

[1]Department of Entomology, University of California, Riverside, CA, U.S.A. and [2]Department of Entomology and Nematology, University of Florida, Gainesville, FL, U.S.A.

Abstract. Evolution of sexual dimorphism in animals has long been of interest to scientists, but relatively few studies have reconstructed evolutionary patterns of extreme sexual dimorphism at a phylogenetic scale, especially in insects. Millipede assassin bugs (Heteroptera: Reduviidae: Ectrichodiinae; 736 spp.) and their sister taxon, Tribelocephalinae (150 spp.), exhibit sexual dimorphism that ranges from limited to extreme, a phenomenon apparently modulated by female morphology. Here, we reconstruct the first phylogeny for the subfamilies Ectrichodiinae and Tribelocephalinae with comprehensive generic representation (152 taxa in 72 genera) using morphological and molecular data (six gene regions). The combined phylogenetic results indicate that Tribelocephalinae are paraphyletic with respect to Ectrichodiinae, and that Ectrichodiinae themselves are polyphyletic. Based on these results, we synonymize Tribelocephalinae with Ectrichodiinae **syn.n.**, describe three new tribes (Ectrichodiini **trib.n.**, Tribelocodiini **trib.n.**, and Abelocephalini **trib.n.**) and two new subtribes (Opistoplatyina **subtrib.n.** and Tribelocephalina **subtrib.n.**), and revise Tribelocephalini **sensu n.** Ancestral state reconstruction of sexual dimorphism reconstructed limited sexual dimorphism in the ancestor of Ectrichodiinae **sensu n.** with at least seven evolutionary transitions to extreme sexual dimorphism within the clade.

This published work has been registered in ZooBank, http://zoobank.org/urn:lsid:zoobank.org:pub:C810E20F-D66A-461F-A0E6-AB1073EA3E3C.

Introduction

The phenomenon of sexual dimorphism has intrigued scientists since Darwin (1859, 1871) with alternative explanations emphasizing differences in reproductive interests or the role of sex-specific ecology and behaviour in shaping divergences between sexes (Roff, 1986; Hedrick & Temeles, 1989; Shine, 1989). Despite the growing body of theoretical and empirical literature exploring sexual dimorphism in animals, including insects at microevolutionary scales (e.g. Lande, 1980; Teder & Tammaru, 2005; Allen *et al*., 2011), relatively few studies have attempted to connect these insights to macroevolutionary levels (e.g. Punzalan & Rowe, 2016). Similarly, studies aimed at reconstructing evolutionary patterns of sexual dimorphism at a phylogenetic scale are comparatively rare across animals (e.g. Oakley, 2005; Binford *et al*., 2016). This is also true for insects, where examples of published studies have made significant contributions towards understanding the evolution of sexually dimorphic horns in scarabaeid beetles (Emlen *et al*., 2005), male clasping and female anti-clasping devices in water striders (Andersen, 1997), sexually dimorphic head shapes in stalk-eyed flies (Baker & Wilkinson, 2001), and body colour sexual dimorphism in damselflies (Cooper *et al*., 2016). In beetles, extreme sexual dimorphism (e.g. larviform females) evolved multiple times from limited sexual dimorphism, resulting in convergent larviform female morphology of distantly related taxa (Bocakova *et al*., 2007; Kundrata & Bocak, 2011). Transitions between limited and extreme sexual dimorphism have otherwise been little studied, and it is unclear if the

Correspondence: Michael Forthman, Department of Entomology and Nematology, University of Florida, 1881 Natural Area Drive, Gainesville, Florida 32611, U.S.A. E-mail: mforthman@ufl.edu

Fig. 1. Images of representative Ectrichodiinae. (A) *Distirogaster* sp. (© 2014 Steve Marshall). (B) *Ectrichodia crux* (Thunberg) (© 2014 Bernard Dupont). (C) *Glymmatophora dimorpha* (de Jonck) (© 2006 Eduard Jendek). (D) *Neoscadra* sp. (© 2010 Melvyn Yeo). (E) *Rhiginia cruciata* (Say) (© 2014 Bonnie Ott). (F) *Schottus* sp. (© 2016 Melvyn Yeo). [Colour figure can be viewed at wileyonlinelibrary.com].

pattern observed in elaterid beetles is also found in other groups of insects.

Millipede assassin bugs (Heteroptera: Reduviidae: Ectrichodiinae) (Fig. 1) are a good study system to investigate evolutionary patterns of sexual dimorphism. Millipede assassin bugs are a diverse group (736 spp., 121 genera; see Forthman *et al*., 2016) of specialist millipede predators (Forthman & Weirauch, 2012) which are predominantly circumtropical in distribution and make up the fifth largest subfamily of assassins bugs (Reduviidae). Members of Ectrichodiinae exhibit sexual dimorphism (Fig. 2) that ranges from slight (e.g. body size, development of the hemelytron, and eye and ocellar size) to extreme, where females exhibit brachyptery to aptery in both pairs of wings and major modifications to the head, thorax and/or legs. Sexual dimorphism can be so extreme that association of conspecific males and females is difficult (e.g. Forthman *et al*., 2016), and males and females have sometimes been described as different species and even as being in different genera (e.g.

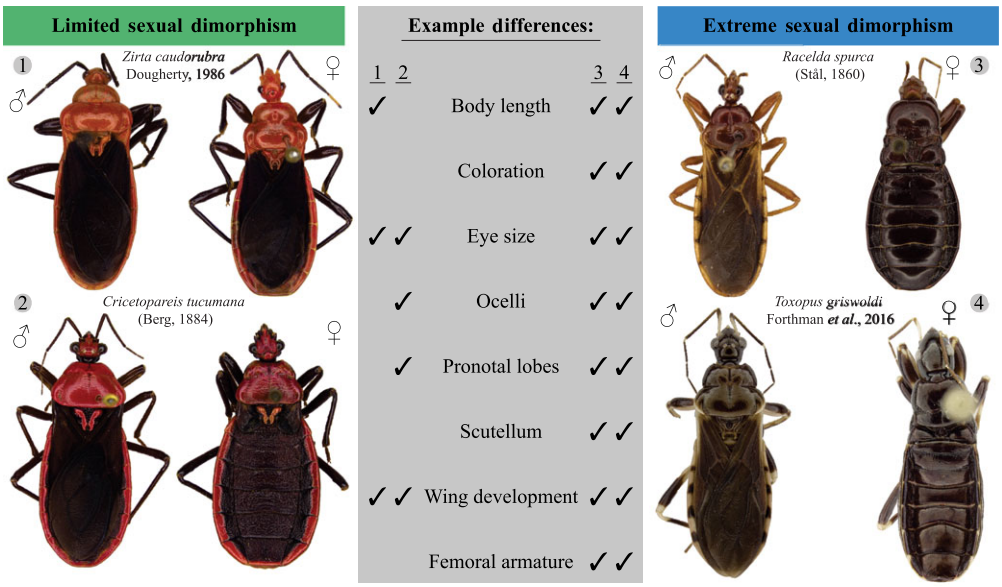

Fig. 2. Examples of limited and extreme sexual dimorphism in Ectrichodiinae species. Numbers in circles correspond to numbers highlighting examples of general morphological differences observed between sexes of the indicated species, but do not reflect how exaggerated the differences may be. Images are not to scale. [Colour figure can be viewed at wileyonlinelibrary.com].

Rédei *et al*., 2012). A preliminary survey of the taxonomic literature on Ectrichodiinae and unpublished observations of available specimens revealed that females are almost always larger than males and have reduced antennal setation compared with males. Approximately half of the surveyed species exhibit some degree of wing reduction in females compared with males, with some species exhibiting wing polymorphism within a given sex, e.g. in some species of *Brontostoma* Kirkaldy or *Glymmatophora* Stål (V. Dougherty, personal observation). Female modifications of the head, thorax and legs may also include a more pronounced gula and a shorter scape, a shorter posterior pronotal lobe and/or a longer and wider anterior lobe, a weakly developed scutellum, stouter fore femora, a larger fossula spongiosa, and tubercles and papillae on the legs that are typically absent in conspecific males. A combination of any of these differences may result in either limited or extreme sexual dimorphism, two terms we define for the present study based on the overall number of morphological differences and the degree to which they differ in males and females of Ectrichodiinae.

Despite the diversity of sexually dimorphic characters and the size of the group, which make Ectrichodiinae a compelling study system, investigations into the evolution of sexual dimorphism are currently impeded by a lack of comprehensive phylogenetic hypotheses for this group. Recent morphological and molecular phylogenetic or phylogenomic analyses of Reduviidae incorporated few representatives of Ectrichodiinae (Weirauch, 2008, 2010; Weirauch & Munro, 2009; Hwang & Weirauch, 2012; Zhang *et al*., 2016), except for a combined morphological and molecular analysis that focused on Madagascan Ectrichodiinae (Forthman & Weirauch, 2016). These studies support Ectrichodiinae (or part thereof; see later) as the sister taxon to Tribelocephalinae, a moderate-sized subfamily (150 species, 16 genera) that comprises mostly cryptically coloured species that display little sexual dimorphism (Maldonado, 1990, 1996; Rédei, 2007; Weirauch, 2010; Ishikawa *et al*., 2015; Davranoglou, 2016; Weirauch *et al*., 2016). Despite the distinctly different overall appearance of members in the two subfamilies, the clade Ectrichodiinae + Tribelocephalinae is supported by several synapomorphies, including the structure of the mandibular and maxillary stylets, subdivided antennal flagellomeres and sexually dimorphic antennal setation (Weirauch, 2008, 2010). Tribelocephalinae are classified into the tribes Opistoplatyini Villiers and Tribelocephalini Villiers, which are separated based on wing venation characters (Villiers, 1943; Maldonado, 1996). The third tribe, Xenocaucini Maldonado, was created for the female-based apterous genus *Xenocaucus* China & Usinger. The recent discovery of a macropterous *Xenocaucus* male with a venation pattern consistent with the diagnosis of Tribelocephalini (Weirauch *et al*., 2016) and the uncertain tribal placement of *Tribelocodia* Weirauch suggest that the tribal classification of Tribelocephalinae is in need of revision.

While most phylogenetic hypotheses support the monophyly of Ectrichodiinae, others found Ectrichodiinae to be paraphyletic with respect to Tribelocephalinae (e.g. Weirauch & Munro, 2009). Similarly, the ectrichodiine species *Ectrichodiella minima* (Valdés) was recovered as sister to the Tribelocephalinae in three of the six equally parsimonious trees in Weirauch's (2010) morphological analysis. Furthermore, the recently described genus *Tribelocodia* shows a mix of characters thought to be diagnostic for both Ectrichodiinae and Tribelocephalinae, and was recovered as part of the Tribelocephalinae in that analysis. More recently, phylogenetic hypotheses in Forthman & Weirauch (2016), based on separate

and combined morphological and molecular data, supported the monophyly of both subfamilies in most analyses, but Ectrichodiinae were rendered paraphyletic with respect to Tribelocephalinae in the parsimony analyses on the molecular dataset. None of the published analyses included an extensive sample of the genus-level diversity of Ectrichodiinae and Tribelocephalinae, and only Forthman & Weirauch (2016) combined morphological and molecular data. A densely sampled, well-resolved and well-supported phylogeny of Ectrichodiinae and Tribelocephalinae is key to investigating the evolution of sexual dimorphism in this group.

Here, we reconstruct the most comprehensive phylogeny of Ectrichodiinae and Tribelocephalinae to date, using separate and combined morphological and molecular analyses to test the monophyly of both subfamilies. Based on our phylogenetic results, we revise the higher-level classification of Ectrichodiinae and Tribelocephalinae. In addition, we use the resulting phylogenetic framework to investigate the evolution of sexual dimorphism with ancestral state reconstruction (ASR) methods. Consistent with hypotheses on the evolution of extreme sexual dimorphism in other groups of insects, we predict that the last common ancestor of Ectrichodiinae and Tribelocephalinae exhibited limited sexual dimorphism, with multiple evolutionary transitions to extreme sexual dimorphism and few reversals to a limited condition.

Material and methods

Taxon sampling

A total of 156 terminal taxa were sampled, comprising 138 Ectrichodiinae representing 62 genera, 14 Tribelocephalinae representing ten genera, and four outgroup species belonging to other subfamilies of Reduviidae. The sample of Tribelocephalinae included genera with controversial tribal placement, such as *Tribelocodia* and *Xenocaucus*, while we emphasized geographic representation and morphological diversity for Ectrichodiinae and included two species of *Ectrichodiella*. The morphological character matrix is based on male specimens, where possible, to minimize the effect of sexually dimorphic character states on phylogenetic reconstruction. However, 28 taxa are represented by females because: (i) some represent mono- or ditypic female-based genera (e.g. *Borgmeierina* Wygodzinsky, *Antiopuloides* Miller) that may be females of male-based species classified in other genera (e.g. *Daraxa* Stål, *Caloundranius* Miller); (ii) the inclusion of female-based genera (e.g. *Schuhella* Dougherty) which permits assignment of undescribed males into existing genera; and (iii) assignment of undescribed females into existing genera (e.g. *Tribelocodia* Weirauch, *Neoscadra* Miller, *Katanga* Schouteden). Of these 28 female-based terminal taxa, we coded male morphology for 12 of these terminals based on taxonomic descriptions, digital images and/or examination of specimens at the Natural History Museum, London, U.K., and/or the American Museum of Natural History, New York, U.S.A. (see table in File S1). A total of 16 terminals lacked information on male morphology because the males remain unknown or the species could not be determined. Despite the possibility of extreme sexual dimorphism in these 16 terminals, we follow Forthman & Weirauch (2016) and infer only male morphological characters that are probably static between males and females (e.g. antennal segmentation, relative lengths of labial segments, scutellar apical processes, etc.) based on existing patterns of sexual dimorphism across Ectrichodiinae and Tribelocephalinae.

Specimens examined for this study are deposited in the following institutions: AM, Australian Museum, Sydney, Australia; AMNH, American Museum of Natural History, New York, U.S.A.; ANIC, Australian National Insect Collection, Canberra, Australia; BMNH, Natural History Museum, London, U.K.; BPBM, Bernice P. Bishop Museum, Hawaii, U.S.A.; CAS, California Academy of Sciences, California, U.S.A.; CNC, Canadian National Collection of Insects, Ontario, Canada; DEI, Deutsches Entomologisches Institute, Müncheberg, Germany; FCAP, Universidade Federal do Pará, Pará, Brazil; MNHN, Muséum National d'Histoire Naturelle, Paris, France; MRAC, Musée Royal de l'Afrique Centrale, Tervuren, Belgium; MTEC, Montana State University, Montana, U.S.A.; QM, Queensland Museum, Brisbane, Australia; SAMC, South Africa Museum, Cape Town, South Africa; SU, Department of Zoology, University of Silesia, Poland; UCR, University of California, Riverside Entomological Research Museum, California, U.S.A.; USNM, National Museum of Natural History, Washington DC, U.S.A.

Morphological methods and data

External morphology was examined using Nikon SMZ1000 and SMZ1500 (Melville, NY, U.S.A.) dissecting microscopes. Mandibular and maxillary stylets and genitalia were dissected from a subset of taxa and examined under a Zeiss Axioscope compound light microscope (Thornwood, NY, U.S.A.) and Nikon SMZ1000 and SMZ1500 microscopes, respectively. For phylogenetic analyses, 168 morphological characters were coded in the Descriptive Language for Taxonomy program (Dallwitz, 1980; Dallwitz *et al*., 1999) using morphological matrices modified from Weirauch (2008, 2010) and Forthman & Weirauch (2016). Additionally, 30 female characters were coded for species in which specimens of both sexes were available or described in taxonomic publications to plot noticeable sex-specific morphological differences on the terminals. One sexual dimorphism character was also coded for ASRs, with limited and extreme sexual dimorphism as the two character states. All morphological characters (199 total) and character states used in this study are given in Table S1. The morphological matrix is provided in File S2. Morphological terminology follows Dougherty (1995), Weirauch (2008), Forero & Weirauch (2012), Hill (2014), and Forthman & Weirauch (2016).

Molecular methods and data

Six gene regions [16S, 18S, 28S D2, 28S D3–D5 rDNA, cytochrome oxidase I (COI) and Wingless (Wg)] were sampled for 59 taxa (47 Ectrichodiinae, nine Tribelocephalinae, three

outgroups) (Table S2). Some relevant sequences deposited in GenBank by Weirauch & Munro (2009), Hwang & Weirauch (2012), Forthman & Weirauch (2016), and Weirauch *et al.* (2016) were combined with new sequence data. Molecular vouchers were associated with a laboratory internal specimen number (RCW prefix), as well as a unique specimen identifier (USI) label that displays specimen information through the Arthropod Easy Capture database (http://www.research.amnh.org/pbi/locality/index.php) and Heteroptera Species Pages (http://research.amnh.org/pbi/heteropteraspeciespage/).

DNA extraction was performed by removing a hind leg and following DNeasy Blood and Tissue Kit protocols (Qiagen, Germantown, MD, U.S.A.). Extracted legs were card-mounted and associated with their respective specimens. For new sequences, PCR was performed using either PuReTaq-Ready-To-Go-PCR-Beads or EmeraldAmp GT PCR Master Mix (GE Healthcare Life Sciences, Pittsburgh, PA, U.S.A.) and T100 Thermal Cyclers [Fisher Scientific (Pittsburgh, PA, U.S.A.) or BioRad (Hercules, CA, U.S.A.)] with protocols listed in Table S3. Primer sequences were obtained from the following sources: those for 16S (16Sa, 16Sb), 18S (18SF, 18SR) and 28S D3–D5 (D3Fa, D5Ra) were taken from Weirauch & Munro (2009); 28S D2 (D2Fa, D2Ra) from Forero *et al*. (2013); COI (C1-J-2183F) from Simon *et al.* (1994) and (C1-N-2609R) Damgaard *et al*. (2000); and Wg (Wg 1A) from Cryan *et al*. (2001) and (Wg DelR1) Urban & Cryan (2007). Amplification was assessed using gel electrophoresis with SyberSafe gel stain and a UV illuminator. PCR products were cleaned using Bioline SureClean (London, U.K.) and sequenced at Macrogen U.S.A. (Sanger sequencing) or on a 3730xl DNA Sequencer at UCR's Institute for Integrative Genome Biology (Applied Biosystems, Carlsbad, CA, U.S.A.). Sequences were assembled and edited in SEQUENCHER v4.8 and are available on GenBank (Table S2).

Each gene region was independently aligned in MAFFT (Katoh & Standley, 2013) using the G-INS-i algorithm. Gene regions were concatenated in SEQUENCEMATRIX v1.7.8. (Vaidya *et al*., 2011) and exported with external gaps coded as question marks (matrix provided in File S3). The best partition scheme and models of sequence evolution were determined using the greedy algorithm and Bayesian information criterion for model selection in PARTITIONFINDER v1.1.1 (Lanfear *et al*., 2012). Each ribosomal gene was treated as a separate subset in the data blocks, while COI and Wg were subdivided into separate codon positions. The resulting partition scheme and models are as follows: *partition 1*: 16S, 28S D2, and 28S D3–D5 (GTR+Γ+I); *partition 2*: 18S, COI codon positions 1 and 2, Wg (GTR+Γ+I); and *partition 3*: COI codon position 3 (HKY+Γ+I).

Phylogenetic analyses

Morphological and molecular datasets were concatenated using MESQUITE v3.04 (Maddison & Maddison, 2015). Separate and combined morphological and molecular phylogenetic analyses were performed using parsimony (TNT v1.1; Goloboff *et al*., 2008), maximum likelihood (ML) (GARLI v2.01; Zwickl, 2006), and Bayesian inference (MRBAYES v3.2.6; Ronquist *et al*., 2012) optimality criteria. For the morphological and combined phylogenetic analyses, the first 168 morphological characters in Table S1 and File S2 were used. Unless otherwise stated, the same parameter settings for a given program were used for all three datasets.

Parsimony

All datasets were subjected to equal weights (EW) parsimony analysis using New Technology search. The combined dataset was also analysed using implied weights (IW), which down-weights characters based on their degree of homoplasy and has been shown to improve support and tree stability (Goloboff, 1993). Internal gaps in the molecular data were treated as fifth state and external gaps as missing data. Prior to analysis, 2661 uninformative molecular characters (out of 4055 characters) were inactivated. Although there is no clear criterion for choosing a particular *k*-value, and the optimal *k*-value is probably matrix-dependent (Goloboff, 1993; Mirande, 2009; Reemer & Ståhls, 2012), we used three concavity constant (*k*) values for IW analysis (3.000000 [default] [IW3], 4.266835 [IW4], and 18.980060 [IW19]) with the latter two based on calculations for average character fit. The use of average character fit to select *k*-values was derived by Mirande (2009) and used by Reemer & Ståhls (2012); this approach selects *k*-values so that the fit/distortion values produced by trees under different *k*-values are divided in regular intervals rather than using a range of regularly distributed *k*-values (Mirande, 2009; Reemer & Ståhls, 2012). We selected average character fit values of 58 and 86% because they encompass a range of *k*-values shown to produce results with the highest similarity to the preferred tree based on various measures of performance (see Reemer & Ståhls, 2012). Default settings for sectorial search, drift and tree fusing were used, the initial driven search level was set at 100 and checked every three hits, the initial addition sequences was set to 14, find minimum length was set to 100 times, and the random seed was set to 4325. Standard bootstrap (BS) resampling with absolute frequencies was conducted with 500 replicates and a New Technology search (initial driven search = 38, check level every three hits, initial addition sequences = 7, find minimum length, ten times).

Maximum likelihood

The ML analyses were conducted using the best partition scheme and models of molecular evolution were determined by PARTITIONFINDER and the Mkv model of morphological evolution (Lewis, 2001). A total of 50 search replicates were performed using random starting trees for each dataset. Nonparametric BS analyses were performed for 500 iterations with the termination condition reduced from 20 000 to 10 000 as recommended in the GARLI manual (Zwickl, 2008).

Bayesian inference

Bayesian analyses used the same partition scheme and models of molecular and morphological evolution as the ML analyses. The following parameters were unlinked so that each partition

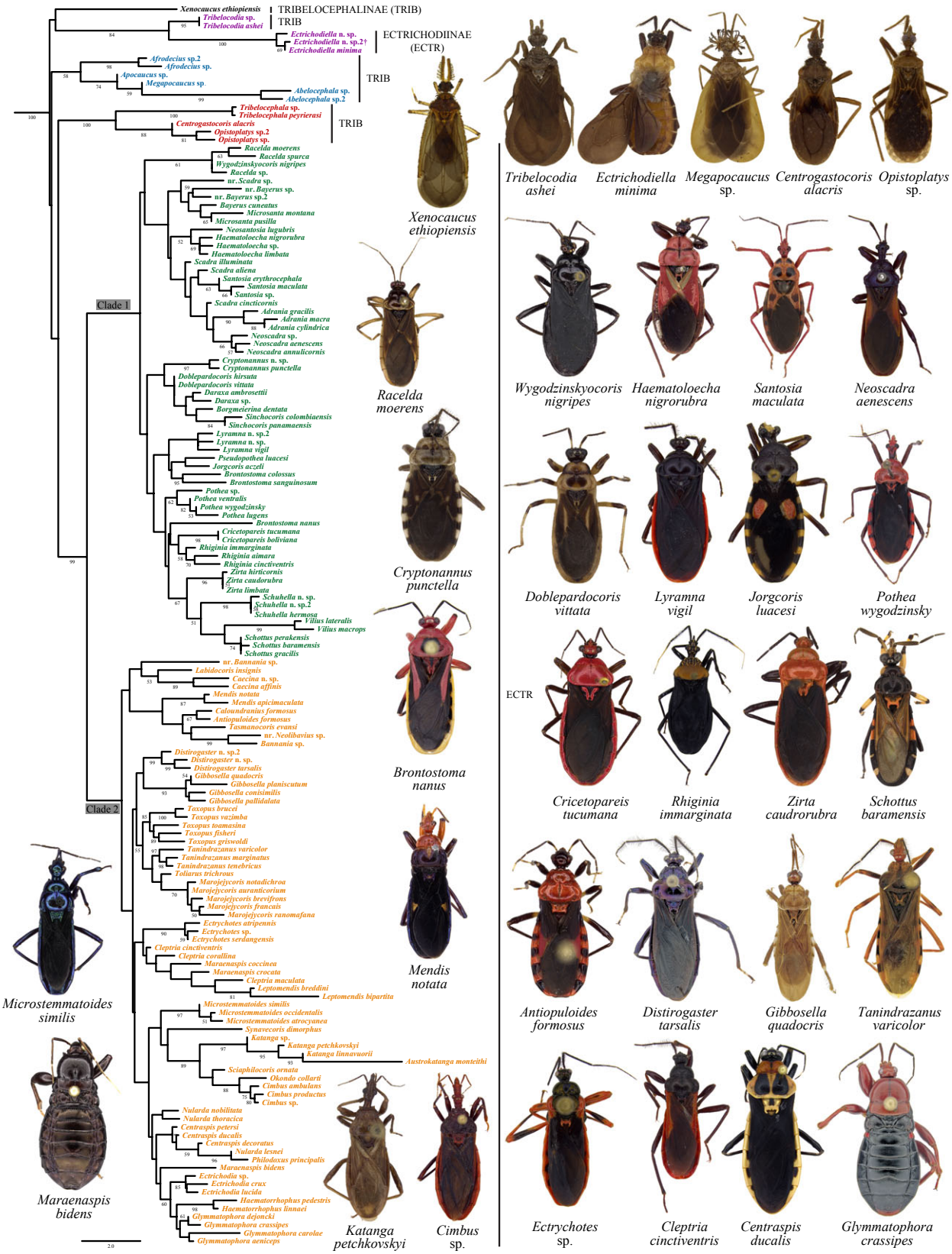

Fig. 3. Legend on next page.

has its own set of parameters: statefeq = (all), revmat = (all), shape = (all) and pinvar = (all). Default priors were used, except for ratepr = variable to allow partitions to evolve under different rates. Two simultaneous runs of 20 million generations were carried out, each with four Markov chain Monte Carlo (MCMC) chains. Parameters and trees were sampled every 20 000 generations, with the first 25% discarded as burn-in. Stationarity was assessed by the average standard deviation of split frequencies (<0.01 for molecular and morphology only datasets; <0.03 for combined dataset) and the potential scale reduction factor (~1.0 for all datasets). Each chain was also assessed for convergence in TRACER v1.6 (Rambaut *et al*., 2014) and possessed combined effective sample size (ESS) values >200 for each parameter after burn-in. The majority-rule consensus tree was generated from the sample of post-burn-in trees in TREEANNOTATER v2.3.2 (Rambaut & Drummond, 2015).

Revised classification of Ectrichodiinae and Tribelocephalinae

We use the combined ML phylogram (Fig. 3) as the basis for our proposed new classification for Ectrichodiinae and Tribelocephalinae because this analysis is derived from the combined dataset, recovers similar higher-level clades as in the parsimony and Bayesian analyses, and is used for ASR analyses for reasons discussed in the next section. We applied two criteria while translating this phylogenetic hypothesis into a new classification: (i) names at the subfamily, tribal, and subtribal levels are only given to taxa that are recovered as monophyletic in the combined analysis [only a single species of *Xenocaucus ethiopiensis* Weirauch *et al*. was included, but Weirauch *et al*. (2016) showed that the eight species of *Xenocaucus* form a clade]; and (ii) suprageneric groupings need to be morphologically diagnosable. Revised diagnoses and re-descriptions for the new subfamily and tribal concepts, as well as for new tribes and subtribes, are provided in the Taxonomy section following the Discussion.

Ancestral state reconstruction of sexual dimorphism

For ASR analysis, the combined ML phylogram was used because it was more resolved than the Bayesian majority-rule consensus tree, and all three phylogenetic approaches recovered similar higher-level relationships. Traditionally, ultrametric trees have been preferred for ASRs based on the argument that phenotypic change is expected to be related to the amount of time elapsed rather than to molecular rates of change along a branch (Bromham *et al*., 2002; Litsios & Salamin, 2012; Cusimano & Renner, 2014). However, some studies have shown correlations between molecular branch lengths and phenotypic change (e.g. Omland, 1997; Smith & Donoghue, 2008); if this is the case, then inferring ASRs on time-calibrated phylogenies could produce inaccurate results as it may not represent the evolution of the species trait appropriately (Litsios & Salamin, 2012). Recently, Litsios & Salamin (2012) and Cusimano & Renner (2014) studied the effects of time-calibrated versus molecular branch lengths on ASRs of continuous and discrete characters, respectively. Based on these studies, there is still no consensus regarding whether ultrametric trees or phylograms produce greater accuracy in ASRs.

Given the potential for branch-length effects on ASRs, we estimated ancestral states on our combined ML phylogram and ultrametric trees. We followed a similar approach to that implemented by Litsios & Salamin (2012) and transformed the phylogram into three ultrametric trees using penalized likelihood in *r8s* v1.70 (Sanderson, 2002, 2003) under the Powell algorithm and different penalties: parametric estimation (penalty = 0), penalty on rate change (penalty = 10) and global molecular clock (penalty = 10 000). Ultrametric trees had a fixed length of 13.53 to match the length of the phylogram. Outgroup taxa were subsequently pruned from all trees in MESQUITE. Although the ML phylogram is completely resolved, *r8s* collapsed eight of the very small, nonzero branch lengths in the generated ultrametric trees. Despite this, we used these trees as generated for ASR as most polytomies are near the terminals, all but one are within clades in which terminals have the same state, and we do not expect major differences with regard to the reconstructions of these nodes on the phylogram.

Sexual dimorphism was coded as either limited (0) or extreme (1) based on the degree and number of differences (six for the extreme condition) observed between sexes. Some taxa, e.g. *Glymmatophora aeniceps* Horváth and *G. dejoncki* Schouteden, exhibit different morphs within males and/or females; when paired with similar morphs, this species will appear to have little sexual dimorphism but will appear extremely sexually dimorphic when paired with different morphs. As such, we coded these terminals as polymorphic for both conditions.

MESQUITE was used for parsimony ASR by tracing characters on the combined ML phylogram, while BAYESTRAITS v2 (Pagel *et al*., 2004) MultiState was used with ML and MCMC approaches on the phylogram and ultrametric trees. For the ML approach, 1000 iterations were performed with rate parameters free or equal, followed by likelihood ratio tests (LTR) to compare the two models; we report ASR results based on restricted rates ($P > 0.09$, df = 1). Under the Bayesian framework, a hyperprior on an exponential distribution drawn from a uniform distribution (interval between 0 and 10) was used. Twenty million

Fig. 3. Maximum likelihood best tree (final ln = −44072.4153) based on 156 taxa (outgroups removed from figure) and a combined morphological and molecular dataset. Molecular data were divided into three partitions and models of sequence evolution: 16S, 28S D2, 28S D3–D5 (GTR+Γ+I); 18S, cytochrome oxidase I (COI) codon positions 1 and 2, Wingless (Wg) (GTR+Γ+I); COI codon position 3 (HKY+Γ+I). Morphological data were analysed under Lewis (2001) Mkv model of morphological evolution. Bootstrap values ≥50 are reported. Branch colours serve as a reference to compare with all other molecular and/or morphological phylogenies in the supplementary materials. Node labels in grey refer to clades discussed in the text. [Colour figure can be viewed at wileyonlinelibrary.com].

generations were conducted with sampling every 2000 generations and the first 25% of generations discarded as burn-in under a free rates and equal rates model. Acceptance rates were between 0.2 and 0.4. Bayes factors (BFs) were calculated to compare results under the free and equal rates models; we report ASR results based on restricted rates (BF < 2). TRACER v1.6 was used to obtain the mean state value for each node, with ESS values >200 for all nodes reconstructed.

Results

Phylogeny of Ectrichodiinae and Tribelocephalinae

Tribelocephalinae were paraphyletic in all analyses, with one of the three Tribelocephalinae lineages recovered in most analyses also including *Ectrichodiella*, and thus rendering Ectrichodiinae polyphyletic. Furthermore, some Tribelocephalinae lineages were more closely related to Ectrichodiinae (excluding *Ectrichodiella*) than to other Tribelocephalinae in most of our analyses. Ectrichodiinae were only monophyletic in the molecular ML and Bayesian analyses (BS < 50 and 92; Figure S1B and C, respectively) that did not include either one of the *Ectrichodiella* terminals coded in the combined analyses. Results of the separate molecular and morphological analyses are given in Figures S1–S3. We report the ML best tree for our combined dataset in Fig. 3, with parsimony and Bayesian results in Figures S4–S6.

Molecular analyses (Figure S1) recovered at least three lineages of Tribelocephalinae with low to high support: *Tribelocephala* + *Opistoplatys*, *Afrodecius* + *Abelocephala*, and *Tribelocodia*. The phylogenetic position of *Xenocaucus* among these Tribelocephalinae lineages remained uncertain, with different analyses recovering this taxon as sister to *Tribelocodia* + *Ectrichodiella* (Fig. 3), sister to *Afrodecius* + *Abelocephala* (molecular only, parsimony, Figure S1A), sister to *Tribelocodia* (molecular only, ML; Figure S1B) or sister to *Abelocephala* + *Megapocaucus* + *Apocaucus* (morphology only, parsimony; Figure S2). In our molecular parsimony analysis (Figure S1A), *Tribelocephala* + *Opistoplatys* was moderately supported as the sister group to an Old World + New World clade ('clade 1') of Ectrichodiinae, rendering Ectrichodiinae paraphyletic. Our molecular ML and Bayesian analyses (Figure S1B and C, respectively) recovered *Tribelocephala* + *Opistoplatys* as sister to a monophyletic Ectrichodiinae (when *Ectrichodiella* is not included) with weak to high support. In the latter analyses, two major Ectrichodiinae clades were recovered with moderate to high support: clade 1 and an Old World clade (clade 2) (Figure S1B, C).

Our morphological parsimony result (Figure S2) was congruent with our molecular results with respect to the tribelocephaline lineages recovered: *Tribelocephala* + *Centrogastocoris* + *Opistoplatys*, *Megapocaucus* + *Apocaucus* + *Afrodecius* + *Abelocephala*, and *Tribelocodia*. However, ML and Bayesian analyses (Figure S3A, B, respectively) supported a paraphyletic Tribelocephalinae with respect to *Ectrichodiella*. *Ectrichodiella* was recovered as the sister group to *Tribelocodia* in all morphological analyses with moderate to high support. Clade 1 and clade 2 were not supported in our morphological analyses, except for a monophyletic clade 1 which was weakly supported in our ML phylogeny; our Bayesian analysis recovered a large polytomy near the base of the remaining Ectrichodiinae.

Higher-level relationships between our combined EW and IW19 parsimony (Figures S4A, S5B, respectively), ML (Fig. 3), and Bayesian (Figure S6) phylogenetic results were largely congruent. The same Tribelocephalinae lineages were recovered in the morphological parsimony and molecular results, with *Ectrichodiella* supported as the sister group to *Tribelocodia*. The *Tribelocephala* + *Centrogastocoris* + *Opistoplatys* clade was weakly supported as the sister group to the remaining Ectrichodiinae, with the exception of our Bayesian phylogeny (unresolved polytomy at the root). In our other IW (IW3 and IW4) parsimony analyses (Figures S4B, S5A), *Tribelocodia* was not monophyletic; *Tribelocodia* sp. was sister to *Xenocaucus*, while *T. ashei* Weirauch was sister to *Ectrichodiella*. In the IW3 parsimony tree (Figure S4B), *Tribelocephala* + *Centrogastocoris* + *Opistoplatys* was sister to *Megapocaucus* + *Apocaucus* + *Abelocephala* with poor support, while *Afrodecius* Jeannel was weakly supported as the sister group to Ectrichodiinae + *Tribelocodia ashei*. In contrast, *Afrodecius* + *Abelocephala* was poorly supported as the sister group to *Tribelocephala* + *Centrogastocoris* + *Opistoplatys* in the IW4 analysis, which, together, were sister to *Megapocaucus* + *Apocaucus*. This larger Tribelocephalinae clade was weakly supported as the sister group to Ectrichodiinae + *Tribelocodia ashei*. With the exclusion of *Ectrichodiella*, the remaining Ectrichodiinae formed a monophyletic group with weak to high support in all combined phylogenies. Clade 2 was recovered in all phylogenetic analyses with low to high support, while clade 1 was recovered in all but the IW phylogenies (paraphyletic with respect to clade 2).

Implications for the classification of Ectrichodiinae and Tribelocephalinae

Based on these phylogenetic results, a new classification for Ectrichodiinae and Tribelocephalinae is proposed (Fig. 4) which synonymizes Tribelocephalinae with Ectrichodiinae (Ectrichodiinae **sensu n.**) and recognizes five tribes within that subfamily: Abelocephalini **trib.n.**, Ectrichodiini **trib.n.**, Tribelocodiini **trib.n.**, Tribelocephalini **sensu n.** and Xenocaucini. (Re)diagnoses, (re)descriptions and discussions are provided in the taxonomy section. Abelocephalini **trib.n.** is proposed to include *Abelocephala* Maldonado, *Afrodecius*, *Apocaucus* Distant, *Enigmocephala* Rédei, *Gastrogyrus* Bergroth, *Homognetus* Bergroth, *Mantangocoris* Miller, and *Megapocaucus* Miller. Ectrichodiini **trib.n.** includes all genera previously classified as Ectrichodiinae, with the exception of *Ectrichodiella*. Tribelocodiini **trib.n.** comprise *Ectrichodiella* and *Tribelocodia.* The concept of Tribelocephalini **sensu n.** is modified to exclude genera now treated as Abelocephalini **trib.n.,** but it now also includes genera traditionally treated

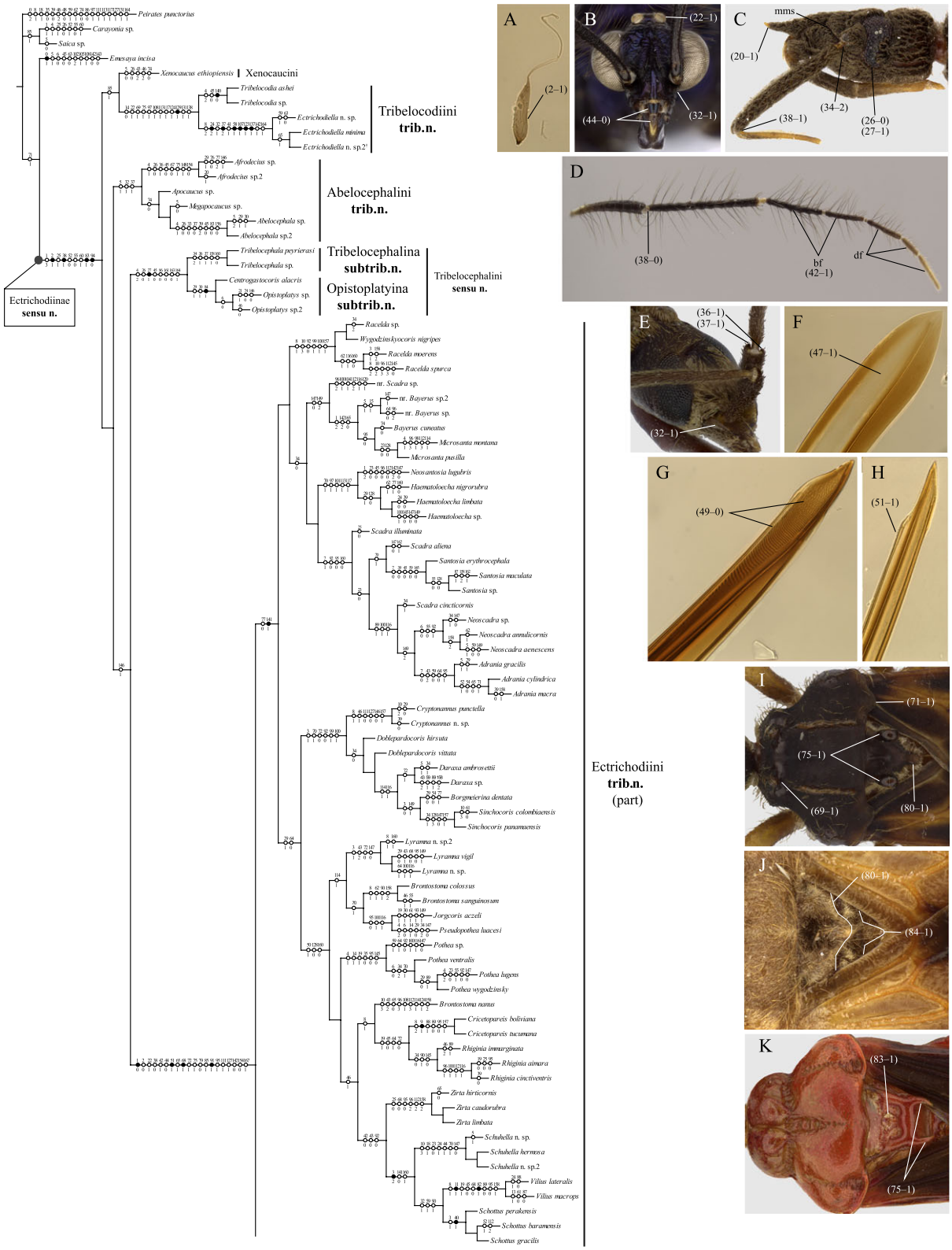

Fig. 4. Legend on page number 585.

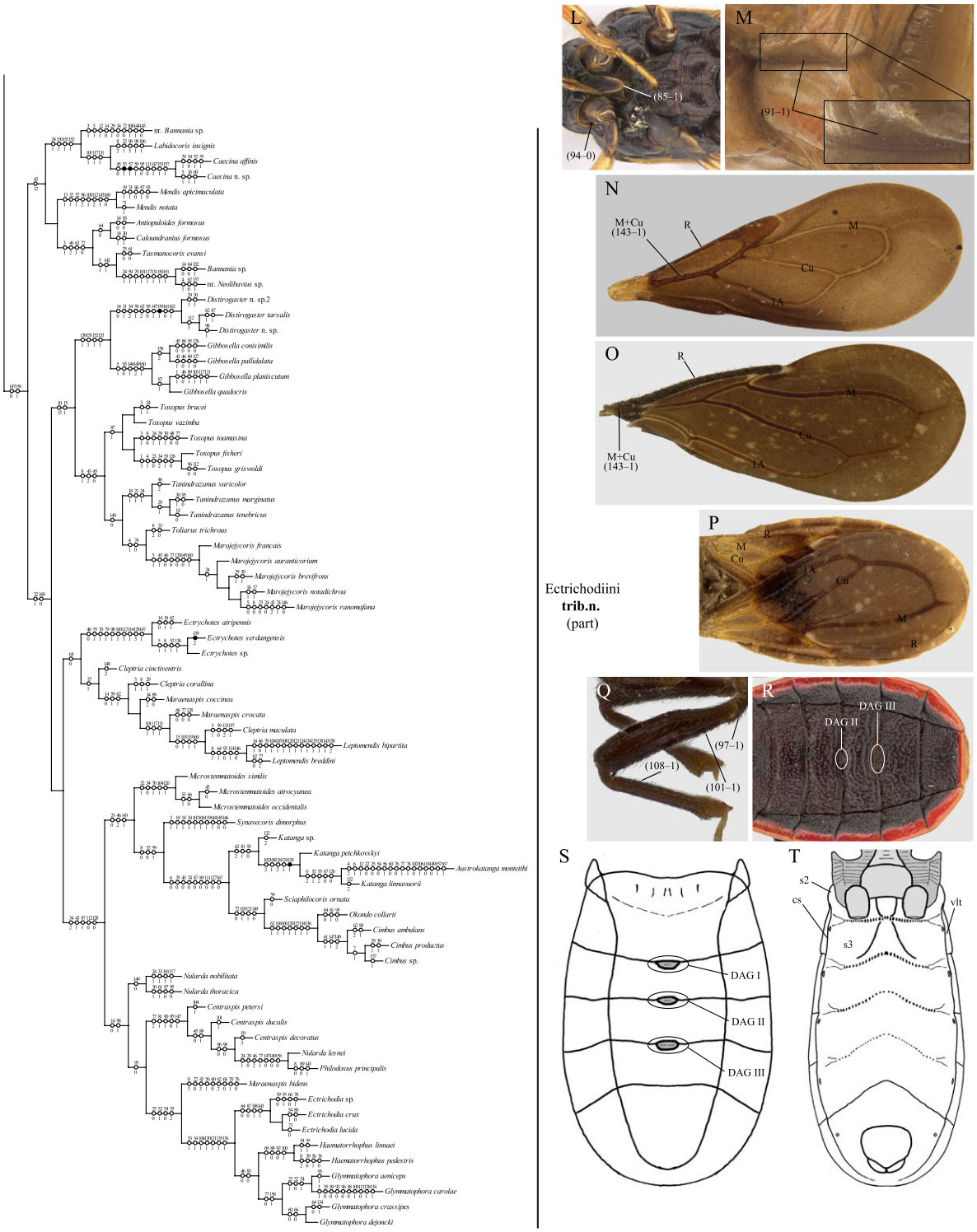

Fig. 4. continued.

as Opistoplatyini. We accordingly create two subtribes in the Tribelocephalini **sensu n.**: Tribelocephalina **subtrib.n.** to accommodate *Tribelocephala* Stål and *Tomolus* Stål, and Opistoplatyina **subtrib.n.**, which comprises genera previously treated as Opistoplatyini, i.e. *Acanthorhinocoris* Miller, *Centrogastocoris* Miller, *Distantus* Villiers, *Opistoplatys* Westwood, *Plectrophorocoris* Miller and *Redeicephala* Davranoglou. Given the uncertain phylogenetic position of *Xenocaucus* in different analyses and the very low support for a *Xenocaucus* + Tribelocodiini **trib.n.** relationship, we decided to retain Xenocaucini as a tribe within Ectrichodiinae.

Evolution of extreme sexual dimorphism

The ML ASR reconstructed limited sexual dimorphism as the ancestral state for Ectrichodiinae **sensu n.** based on the combined ML phylogram (Fig. 5). At least seven independent transitions from limited to extreme sexual dimorphism were reconstructed within the clade, with a single reversal to limited sexual dimorphism reconstructed in the Tribelocodiini **trib.n.** These results were congruent with ML reconstructions on ultrametric trees (Table S4) and all MCMC reconstruction (Table S4). They were also largely identical with the parsimony-based ASR, except that this reconstruction did not hypothesize any reversals (Figure S7).

Plotting sexually dimorphic characters at the terminals (Fig. 5) revealed that taxa exhibiting limited sexual dimorphism were generally characterized by one to three minor differences between males and females. These morphological differences often included a reduction in the female's eye size, wing development (brachypterous, micropterous or apterous) and associated changes in pronotal lobe lengths. Other taxa may exhibit minor differences in other pronotal features, as well as leg and abdominal features. However, in all cases, the presence or absence of the ocellar lens, postclypeal surface, presence or absence of the antennal shield, anterior pronotal width and scapus length, and presence or absence of paramedian abdominal sternal carinae did not differ between sexes.

Taxa exhibiting only extreme sexual dimorphism tended to have at least six drastic differences between sexes. In these species, the extreme condition was often characterized by apterous females, with severe changes in pronotal dimensions or, more often, the dimensions of the pronotal lobes. Eyes were generally reduced or represented only by scattered ommatidia (e.g. *Xenocaucus*). Where ocelli were present in males, these were drastically reduced or absent in the females. In several taxa, males had a depressed postclypeus and well-developed paramedian scutellar processes (e.g. *Distirogaster* Horváth), but females exhibited a flat postclypeus and weakly developed scutellar processes. Females could also have increased leg armature (tubercles and/or papillae) and reduced abdominal features.

Discussion

Multiple transitions from limited to extreme sexual dimorphism

Our study supported multiple evolutionary transitions to extreme sexual dimorphism during the evolution of modern Ectrichodiinae **sensu n**. Based on our results and observations of other species, extreme sexual dimorphism is apparent in taxa that have macropterous males and apterous or micropterous females (e.g. *Xenocaucus*, *Toxopus* Forthman *et al*., *Distirogaster*). Compared with males, females generally show drastic reductions in several head, thoracic and abdominal features, while anterior pronotal lobe enlargement and additional leg armature are observed. Given the convergence of these characters in distantly related taxa, we caution the use of female characters in phylogenetic reconstruction and taxonomic decisions [e.g. see Rédei & Tsai, 2012 (*Haematoloecha puetzi* (Kerzhner & Günther))], especially for known or potentially (i.e. where both sexes are currently unknown) extremely dimorphic species. Phylogenetic studies on cantharoid and elateroid beetles, where previous higher-level classification was primarily based on characters that have been shown to be highly homoplastic among lineages with neotenic females, have reached similar conclusions (see Bocakova *et al*., 2007; Bocak *et al*., 2008; Kundrata & Bocak, 2011).

Our dataset was coded at the species level for which males or females for several included species are unknown, or conspecificity of males and females of undescribed species is unclear. Sexual dimorphism data were therefore missing for many taxa, potentially underestimating the number of transitions between limited and extreme sexual dimorphism in the group. For example, both described species of *Apocaucus* are known

Fig. 4. Combined morphological and molecular maximum likelihood (ML) topology (converted to cladogram) showing new classification of Ectrichodiinae **sensu n.** (see Fig. 3 for comparison to old classification). Unambiguous character optimizations are shown. (A) *Tribelocephala* sp. Bulbous trichome. (B) *Distriogaster tarsalis*. Head, rostral view. (C) *Tribelocephala* sp. Head, lateral view. (D) *Toxopus insignis*. Antenna, lateral view (modified from Forthman *et al*., 2016). (E) *Afrodecius* sp. Head and scapus, dorsolateral-rostral view. (F) *Rhiginia cinctiventris*. Apex of mandibular stylet. (G) *Centraspis ducalis*. Apex of right maxillary stylet. (H) *Rhiginia cinctiventris*. Apex of left maxillary stylet. (I) *Ectrichodiella* sp. Thorax, dorsal view. (J) *Centrogastocoris alacris*. Scutellum and postscutum, dorsal view (K), nr. *Bannania* sp. Thorax, dorsal view. (L) *Tanindraanus* sp. Thorax, ventral view (modified from Forthman *et al*., 2016). (M) *Tanindrazanus varicolor*. Metathoracic gland evaporatorium, lateral view. (N) *Ectrichodiella minima.* Right hemelytron, dorsal view. (O) *Tribelocephala* sp. Right hemelytron, dorsal view. (P) *Centrogastocoris alacris*. Hemelytra, dorsal view. (Q) *Ectrichodiella minima*. Foreleg, anterior view. (R) *Cricetopareis tucumana*. Dorsal abdominal glands, dorsal view. (S) *Ectrichodiella minima*. Dorsal abdominal glands, dorsal view. (T) *Tanindrazanus varicolor*. Abdomen, ventral view. Character numbers and character state codings are listed in Table S1. Abbreviations used in figures: 1A, first anal vien, bf, basiflagellomere; cs, ventral connexival suture; Cu, cubitus; DAG I/II/III, dorsal abdominal gland I/II//III; df, distiflagellomere; M, media; mms, suture separating mandibular and maxillary plates; R, radius; s2, abdominal sternite II (fused sternites I and II); s3, abdominal sternite III; vlt, ventral laterotergite III. [Colour figure can be viewed at wileyonlinelibrary.com].

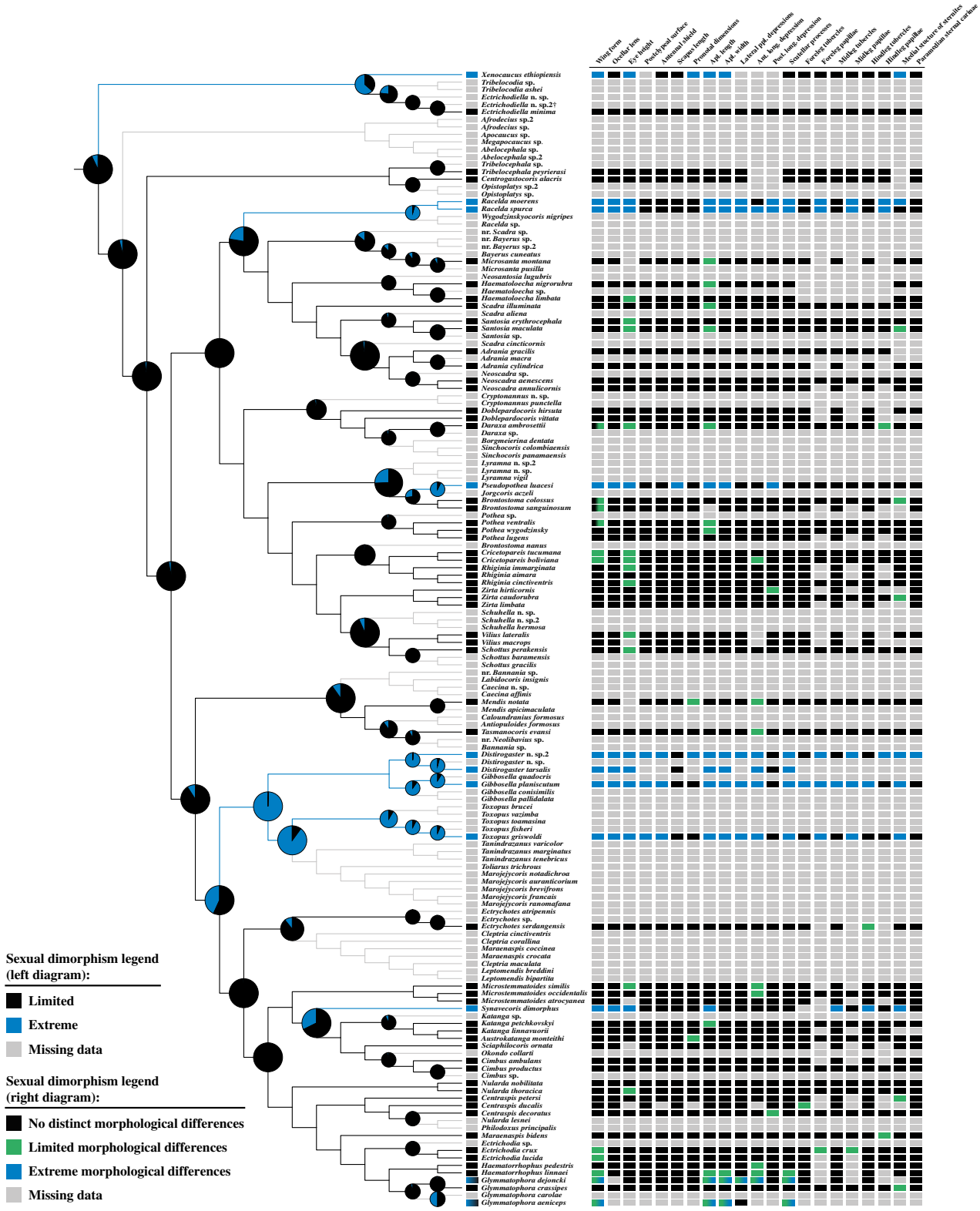

Fig. 5. Legend on next page.

only from macropterous males, but we examined apterous putative females, suggesting the possibility of extreme sexual dimorphism in *Apocaucus*. We have observed similar situations in other taxa, e.g. *Tribelocodia*, *Lyramna* Breddin, and many other species of *Gibbosella*. In addition, described species may have not been associated correctly because of extreme sexual dimorphism; for example, *Parascadra breuningi* Kerzhner & Günther was shown to be the micropterous female of *Rhysostehus glabellus* Hsiao (see Rédei *et al*., 2012). We suspect that similar taxonomic issues are widespread in Ectrichodiinae **sensu n.** given that more than half of the genera are monotypic and based on one or few individuals of a single sex. Molecular data are currently unavailable for these taxa, but could assist in testing putative conspecificity (e.g. Weirauch *et al*., 2016).

Wing reduction and/or extreme sexual dimorphism in females is documented in many other insect orders, such as Diptera (Disney, 1996), Phasmatodea (Whiting *et al*., 2003), Hemiptera: Coccoidea (Gullan & Kosztarab, 1997) and Strepsiptera (Kathirithamby, 1989), and hypotheses have been proposed to explain the evolution of this phenomenon, focusing on either different reproductive interests in males and females or sex-specific ecology and behaviour (Hedrick & Temeles, 1989; Shine, 1989). One hypothesis tied to reproductive interests posits that the reduction of wings (and other morphological features) permits reallocation of resources to increased fecundity in females and/or reduces the age of first reproduction (Darwin, 1859; Roff, 1986; Denno *et al*., 1989; Roff & Fairbairn, 1991). A second compatible hypothesis is that these species are under less selection pressure to maintain dispersive flight capabilities in stable environments (Slater, 1977; Roff, 1990). Brachypterous and apterous morphs of millipede assassin bugs are commonly observed in leaf litter microhabitats which may qualify as stable environments, especially in tropical rainforests, compared with macropterous morphs that fly in open vegetation (V. Dougherty, personal observation). Furthermore, brachypterous and apterous females generally have larger femora that are sometimes modified with additional armature, as well as a larger pronotum and/or anterior pronotal lobe. The modifications in these two structures may be correlated with each other, which may be used to subdue larger prey items for greater nutrition and increased egg production. However, experimental evidence on allocation trade-offs between flight and reproduction are lacking for Ectrichodiinae **sensu n.** Regardless, trade-offs between the production of morphological features for dispersive flight and increased reproduction and the role of stable habitats are plausible hypotheses to explain the evolution of wing reduction (and other leg and thoracic modifications) and extreme sexual dimorphism in this group of insects. A third hypothesis states that flight capabilities are reduced in taxa that occupy isolated habitats (e.g. oceanic islands, caves, mountaintops), as dispersers are likely to experience higher risks of mortality (Darwin, 1859; Wagner & Liebherr, 1992). Under this hypothesis, we would expect both sexes in a species to exhibit the same wing and associated thoracic reductions, which is the case in some Ectrichodiinae **sensu n.** taxa (e.g. *Maraenaspis* Karsch, *Haematorrhophus* Stål); however, the isolation hypothesis would not explain sex-specific morphological reductions as they are commonly observed in Ectrichodiinae **sensu n.**

Phylogenetics and reclassification of Ectrichodiinae and Tribelocephalinae

Previous phylogenetic hypotheses across Reduviidae (Weirauch, 2008; Weirauch & Munro, 2009; Hwang & Weirauch, 2012; Zhang *et al*., 2016) supported the clade we recognize here as the subfamily Ectrichodiinae **sensu n.** (including Tribelocephalinae), which was also well supported in all of our current analyses. In contrast, these earlier analyses lacked adequate taxon and character sampling to reconstruct relationships within Ectrichodiinae **sensu n.**, specifically testing the hypotheses that the two former subfamilies, Ectrichodiinae and Tribelocephalinae, are not reciprocally monophyletic [Weirauch & Munro, 2009 (in part); Weirauch, 2010]. Our phylogenetic results utilized a much more comprehensive sample of Ectrichodiinae **sensu n.**; we used the results of our combined morphological and molecular ML phylogenies to reclassify the clade into diagnosable monophyletic groups (Fig. 4).

Taxonomy

Ectrichodiinae Amyot & Serville sensu n.
(Fig. 4A–T)

Ectrichodiinae Amyot & Serville, 1843, 1: 342. Type genus: *Ectrichodia* Lepeletier & Serville, 1825, 10: 279.

Tribelocephalinae Stål, 1865, 3: 44. **New synonymy.** Type genus: *Tribelocephala* Stål, 1853, 10: 263.

Diagnosis. Male. Recognized by the subdivided antennal basi- and/or distiflagellomeres making the antennae appear five- to eight-segmented (Fig. 4D) (four-segmented in *Neozirta*

Fig. 5. BAYESTRAITS MultiState maximum likelihood (ML) reconstruction of ancestral sexual dimorphism states on the ML phylogram (Fig. 3) for Ectrichodiinae **sensu n.** (tree converted to cladogram for visual). On the left, sexual dimorphism for terminal taxa is coded as limited (black), extreme (blue), polymorphic (gradient blue and black) or missing data (grey). Pie charts at select nodes show probability values from the ML reconstructions; branches are coloured to reflect the highest probability of a colour state at that branch; grey internal branches indicate ambiguity in reconstructions. On the right, colour codes correspond to Fig. 2, with characters that exhibit no noticeable differences (black), differences in limited sexual dimorphism (green) or differences in extreme sexual dimorphism (blue) between males and females shown for species in which data on both sexes are known. For taxa that exhibit limited sexual dimorphism, individuals of a sex that exhibit no or minor differences (i.e. polymorphic) are coded gradient black and green. For taxa exhibiting both limited and extreme sexual dimorphism (i.e. males and/or females have different morphs), differences are indicated with gradient green and blue. Missing data are indicated in grey. [Colour figure can be viewed at wileyonlinelibrary.com].

Distant, *Schottus* Distant, *Schuhella* Dougherty, *Tribelocodia*, *Vilius* Stål, *Xenorhyncocoris* Miller and *Zirta* Stål), more than 35 external transverse ridges on the mandibular stylet (47–1; Fig. 4F), lamellate ventral processes on the right maxillary stylet interiorly (49–0; Fig. 4G) (tooth-like in *Vilius*), a medially depressed scutellar disc (83–1; Fig. 4K) (flat in some genera, e.g. *Abelocephala*, *Glymmatophora* and *Haematorrhophus*), and a globular forecoxa (94–0; Fig. 4L). *Female.* Similar to male with respect to features mentioned in diagnosis; apterous to macropterous; external genitalia short, plate-like; may exhibit drastic reductions in morphology compared with conspecific males if wing condition different from that of the male.

Redescription. Male. Structure, head: short or elongate, variably shaped; scapus and pedicellus with long, dense, erect to semi-erect setae; antennal flagellomeres five- to eight-segmented with the exception of four-segmented antenna in *Schottus*, *Schuhella*, *Tribelocodia*, *Vilius* and *Zirta*; labium with three visible segments (segments II–IV; segment I reduced); mandibular stylet with more than 35 transverse ridges on external surface; right maxillary stylet with interior lamellate ventral processes (tooth-like in *Vilius*). Thorax: scutellar disc medially depressed; globular coxae; hemelytron, when present, with two to three membranal cells (one in *Quinssyana funeralis* Distant). Abdomen: dorsal laterotergites separated from mediotergites by membrane; ventral laterotergites separated from mediosternites by membrane (except for segment II in Ectrichodiini **trib.n.**); mediosternites fused. *Female*. Similar to male but generally larger in size (except in, e.g., *Abelocephala* and *Afrodecius*); scapus and pedicellus with short, sparse, erect to semi-erect setae in Ectrichodiini **trib.n.**; compound eyes present but may be reduced in size; ocelli present or absent; anterior pronotal lobe variable in length and width with respect to posterior pronotal lobe; scutellum may be reduced; hemelytron apterous to macropterous; legs sometimes with papillae on trochanters and femora; fossula spongiosa typically larger than males relative to tibial length; external genitalia short, plate-like.

Comments. A taxonomic history of Ectrichodiinae prior to our study is provided by Dougherty (1995). No tribal classification has been proposed for this subfamily before. Prior to this reclassification, Ectrichodiinae was diagnosed by the following features: subdivided basi- and/or distiflagellomeres, making the antennae appear more than four-segmented; presence of ventral and dorsal processes on the left maxillary stylet; bifurcated scutellum; hemelytral membrane with two or three cells; fossula spongiosa on foretibia, as well as midtibia in many species; absence of the ventral connexival suture on abdominal sternite II; Brindley's gland and associated evaporatorium present, and three dorsal abdominal glands (DAGs) with DAG III ostioles larger than those of DAGs I and II.

The subfamily Tribelocephalinae was first recognized as a subfamily of Reduviidae by Stål (1865) and was subsequently divided by Villiers (1943) into two tribes based on venation patterns of the hemelytron: Opistoplatyini and Tribelocephalini. A third tribe, Xenocaucini, was later erected by Maldonado (1996) for the female-based genus *Xenocaucus* characterized by several unique features among Tribelocephalinae. Species of Tribelocephalinae have been characterized by less globular eyes, a long first visible labial segment, the strongly bent scapo-pedicellar articulation, the very small corium compared to the large membranous area of the hemelytron, and the presence of dense vestiture that included trichomes with a bulbous base and thin, curved apex. All species included in this subfamily lack ocelli, except for *Tribelocodia*.

As mentioned, previous phylogenetic results have provided consistent support for Ectrichodiinae **sensu n.**, with some of the morphological synapomorphies from these studies (Weirauch, 2008, 2010) supported by our results. However, the monophyly of both former subfamilies remained doubtful, and our phylogenetic results confirm their nonmonophyly. As such, we synonymize Tribelocephalinae with Ectrichodiinae, erect three new tribes and two subtribes, and revise the tribe Tribelocephalini. We also include Xenocaucini as a tribe in Ectrichodiinae **sensu n**. In addition to the characters listed in the diagnosis, our character optimizations recovered additional synapomorphies: very dense vestiture with bulbous hairs present on the integument (absent in the Ectrichodiini), eye more than one-half of the head height (reduced in many apterous species or in females), pedicellus ventrally inserted on scapus so that pedicellus and flagellomeres point posteriorly (absent in the Ectrichodiini), pronotum wider than long (exceptions observed in a number of taxa), anterior pronotal lobe shorter than the posterior lobe (exceptions observed in a number of taxa, particularly in individuals with reduced wings), and lateral depression present on the posterior pronotal lobe (absent in some apterous individuals). As our ASR results show, extreme sexual dimorphism has evolved multiple times in this subfamily, with females showing varying degrees of reductions to the overall morphology compared with conspecific males.

Abelocephalini trib.n.

http://zoobank.org/urn:lsid:zoobank.org:act:A0FFB295-066B-42A7-909F-666DB9305F97
(Fig. 4E)

Type genus. Abelocephala Maldonado, 1996, 98: 140.

Diagnosis. Male. Diagnosed by the presence of bulbous trichomes (2–1; Fig. 4A), eye reniform with concave posterior margin, ocelli absent, antennal shield present (32–1; Fig. 4B, E), scapus with ventroposterior apical lobe (37–1; Fig. 4E) (absent in *Abelocephala*), pedicellus ventrally inserted on scapus so that pedicellus and flagellomeres point posteriorly (38–1; Fig. 4C), posterolateral margin of pronotum surpassing medial pronotal margin (71–1; Fig. 4I), scutellum with well-developed medial process (80–1; Fig. 4I, J) (paramedian process also present in *Afrodecius*), tibiae lacking fossula spongiosa, tarsi two-segmented, hemelytron greatly surpassing abdominal apex, proximal part of M and Cu of hemelytron forming one vein

(143–1; Fig. 4N, O). *Female*. Based on Ishikawa *et al*.'s (2015) redescription of *Abelocephala* and females personally observed and assigned to *Apocaucus* and *Afrodecius* (but not to any described species), similar to features given in the male's diagnosis, except eyes slightly reduced and apterous to brachypterous. In addition, pronotum more quadrate (trapezoidal in male) and scapus thicker.

Description. Male. Vestiture: dense vestiture on parts of the head, anterior to lateral margins of the pronotum, and near the thoracic-abdominal articulation; bulbous trichomes present. Structure, head: clypeus without anterior process; ocelli absent; antennal shield present; scapus with ventroposterior apical lobe (except in *Abelocephala*), pedicellus ventrally inserted on scapus so that pedicellus and flagellomeres point posteriorly; pedicellus strongly curved; distinct constriction between postocular region and neck; labrum completely sclerotized. Thorax: posterolateral margin of pronotum surpassing medial pronotal margin; scutellum with well-developed medial process (paramedian process also present in *Afrodecius*); tibiae lacking fossula spongiosa; tarsi two-segmented; hemelytron greatly surpassing abdominal apex; proximal part of M and Cu of hemelytron forming one vein. Abdomen: DAGs II and III ostioles only present and of similar size in adults. *Female.* Similar to male except apterous to brachypterous, thicker scapus, smaller eyes, more quadrate pronotum, and thicker femora and tibiae.

Comments. Abelocephala, *Afrodecius*, *Apocaucus* and *Megapocaucus* are included within this tribe based on our phylogenetic results. Based on our diagnosis, we also include *Enigmocephala*, *Gastrogyrus*, *Homognetus* and *Mantangocoris*. Rédei (2007) highlighted the morphological similarities between *Enigmocephala* with *Gastrogyrus*, *Mantangocoris* and *Afrodecius*, particularly with head morphology (e.g. the anteriorly declivent head, pubescent postocular and gular regions, robust labium and/or apical processes on ultimate labial segment). *Homognetus* is also similar to these genera in the pubescent postocular and gular regions. It is worth noting that the male of *Xenocaucus ethiopiensis* was observed for our analysis and also exhibits many of the same diagnostic features of this tribe (e.g. two-segmented tarsus; hemelytron greatly surpassing abdominal apex), as well as other morphological features (fringe of hairs on postocular and gular areas; DAGs II and III ostioles of similar size). Thus, it is possible that this genus may be a member of Abelocephalini and was recovered as sister to or nested within this tribe in some of our phylogenetic results; however, further phylogenetic testing is needed with more representatives of this tribe for both molecular and morphological data.

Ectrichodiini trib.n.

http://zoobank.org/urn:lsid:zoobank.org:act:260E2B31-E6E1-41C6-BE9E-71FF068D20EC
(Fig. 4A, D, F–H, K–M, R, T)

Type genus. Ectrichodia Lepeletier & Serville, 1825, 10: 279.

Diagnosis. Male. Diagnosed by the absence of bulbous trichomes; the distally or slightly ventrally inserted pedicellus (38–0; Fig. 4D); basiflagellomere subdivided into two pseudosegments (42–1; Fig. 4D) (not subdivided in *Schottus*, *Schuhella*, *Vilius* and *Zirta*); a subdivided labrum (44–0; Fig. 4B) (not subdivided in *Schuhella*); the ventral, internal row of processes on the left maxillary stylet (51–1; Fig. 4H); paramedian scutellar processes present (75–1; Fig. 4K); a long prosternal stridulatory process that surpasses the posterior margin of the forecoxal cavity (85–1; Fig. 4L); the metathoracic gland evaporatorium as modified cuticle (91–1; Fig. 4M); and the absence of the ventral connexival suture on abdominal sternites II (154–0; Fig. 4T). *Female.* Similar to male diagnostic features, but apterous to macropterous, antennal setation shorter, and scutellum may be reduced.

Description. Male. Vestiture: glabrous to dense, erect to semi-erect vestiture without bulbous trichomes. Structure, head: ocellar lens in, at least, macropterous individuals; pedicellus distally or slightly ventrally inserted in scapus; basiflagellomere typically subdivided into two pseudosegments (one-segmented in *Schottus*, *Schuhella*, *Vilius* and *Zirta*); labrum subdivided by transverse membrane (completely sclerotized in *Schuhella*); left maxillary stylet with ventral, internal row of processes. Thorax: macropterous forms, at least, with a distinct longitudinal depression on the posterior pronotal lobe; posterolateral margin of pronotum not or barely surpassing medial pronotal margin; paramedian scutellar processes present; prosternal stridulatory process long, surpassing posterior margin of forecoxal cavity; metathoracic gland evaporatorium present as modified cuticle; tarsi three-segmented. Abdomen: ventral connexival suture on abdominal sternites II absent; DAGs II and III ostioles present in adults (DAG II ostioles absent in some species; see Discussion), with DAG III larger than DAG II. *Female.* Similar to male except apterous to macropterous; shorter antennal setation; eyes, ocelli and scutellum may be reduced; pronotum similar to male or differs in overall pronotal dimension or dimensions between the lobes; femora may be more incrassate and bear papillae ventrally; fossula spongiosa typically larger than male.

Comments. All genera recognized in the previous classification of Ectrichodiinae, with the exception of *Ectrichodiella*, are included in the Ectrichodiini. Several other synapomorphies of the nominal tribe were recovered in our optimizations, but show reversals or modifications in some of the included taxa. The absence of a single medial scutellar process (79–0) is optimized on our phylogeny, however some genera (e.g. *Ectrychotes* Burmeister) have very small medial processes. Many genera and species are characterized by more incrassate forefemora compared to the mid femora (95–1), but a number of other genera and species have slender legs (e.g. *Tanindrazanus* Forthman *et al*., *Pothea* Amyot & Serville). A fossula spongiosa is commonly observed on the fore- and mid tibiae (111–1, 127–1), but there are several instances of reversals on one or

both legs. Although DAGs II and III ostioles are present in many of the species we have observed (Fig. 4R), as well as by Weirauch (2006), some species in *Scadra* Stål, *Pseudopothea* Wygodzinsky, *Microsanta* Breddin, and *Adrania* Stål, lack DAG II ostioles.

Tribelocodiini trib.n.

http://zoobank.org/urn:lsid:zoobank.org:act:2FAF59BF-8F90-4829-93E9-CE2B71B006FE
(Fig. 4I, N, Q, S)

Type genus. Tribelocodia Weirauch, 2010, 41: 106.

Diagnosis. Male. Recognized by the narrow postocular shape in dorsal view (14–0); presence of ocelli (22–1; Fig. 4B); pedicellus ventrally inserted on scapus so that pedicellus and flagellomeres point posteriorly (38–1; Fig. 4C); pronotal transverse furrow laterally divided by elevated cuticle (69–1; Fig. 4I), which is distinctly ridge-like in some *Ectrichodiella* spp.; posterolateral margin of pronotum surpassing medial pronotal margin (71–1; Fig. 4I); scutellum with paramedian scutellar processes and a well-developed medial process (75–1, 80–1; Fig. 4I); small tubercles uniformly covering the trochanters, femora and tibiae (97–1, 101–1, 108–1, 113–1, 117–1, 124–1, 129–1, 131–1, 138–1; Fig. 4Q); tibiae lacking fossula spongiosa; and proximal parts of M and Cu of forewing forming one vein (143–1; Fig. 4N). *Female.* Diagnostic features as in male, except in *Tribelocodia*, postocular shape is broader in dorsal view, ocelli absent, pronotal transverse furrow reduced (pronotal lobes indistinct), pronotum transversely ovoid, scutellum and scutellar processes reduced, and apterous. Females belonging to *Tribelocodia* can be easily identified by the fused tibiotarsus on all legs and diminutive pretarsal claws, which are also observed in males of this genus.

Description. Male. Structure, head: clypeus without anterior process; postocular narrow in dorsal view; eye reniform with concave posterior margin; ocelli present; pedicellus ventrally inserted on scapus so that pedicellus and flagellomeres point posteriorly; pedicellus moderately to strongly curved; basiflagellomere one-segmented; constriction between postocular region and neck; labrum sclerotized. Thorax: pronotum with transverse furrow subdivided by laterally elevated cuticle, ridge-like in *Ectrichodiella*; posterolateral pronotal margin surpassing medial pronotal margin; metepisternal supracoxal lobe of mesocoxal cavity present; scutellum with well-developed paramedian processes and a well-developed medial process; trochanters, femora and tibiae with small, uniformly distributed setigerous tubercles; tibiae lacking fossula spongiosa; tarsi two-segmented in *Ectrichodiella*, one-segmented and fused with tibia in *Tribelocodia*; pretarsus distinct in *Ectrichodiella*, diminutive in *Tribelocodia*; proximal parts of M and Cu of forewing forming one vein. Abdomen: DAGs I–III ostioles present in adults (except I absent in *Tribelocodia*) and of similar sizes. *Female.* Similar to the features described in the male except, within *Tribelocodia*, apterous, postocular broad in dorsal view, ocelli absent, pronotal transverse furrow reduced, resulting in indistinct pronotal lobes indistinct, pronotum rounded and scutellum reduced.

Comments. This tribe includes the Neotropical genera *Ectrichodiella* and *Tribelocodia*. Conspecific males and females of *Ectrichodiella* appear very similar. While conspecific males and females of *Tribelocodia* remain unknown, we have observed one undescribed female assigned to this genus which exhibits drastic morphological reductions in morphology.

Tribelocephalini Villiers sensu n.
(Fig. 4C, J, O, P)
Tribelocephalini Villiers, 1943, 10: 9. **(partim)**.
Opistoplatyini Villiers, 1943, 10: 9. **New synonymy**.

Type genus. Tribelocephala Stål, 1853, 10: 263.

Diagnosis. Male. Distinguished by the dense, tomentose vestiture throughout the body (especially the entire head) (Fig. 4C), head longer than pronotum (except a little shorter than pronotum in *Tomolus*), clypeus with anterior process (20–1; Fig. 4C) (absent in *Opistoplatys* Westwood and *Tomolus*), eye adpressed closely to the head surface and with concave anterior and posterior eye margin (26–0, 27–1; Fig. 4C) (concavity slight in *Tomolus*), ventral margin of second visible labial segment (appears dorsal when retracted under the head) is straight or concave (45–0), apex of short prosternal stridulatory process acute (86–0), and DAGs I–III ostioles present in adults and of similar sizes (164–1; Fig. 4S). *Female*. Similar to male, but hemelytron sometimes reaching anterior margin of tergite VII but not reaching abdominal apex and abdomen typically wider.

Redescription. Male. Vestiture: dense tomentose vestiture throughout the entire body, bulbous trichomes present. Structure, head: head longer than pronotum (a little shorter than pronotum in *Tomolus*); clypeus with anterior process (absent in *Opistoplatys* and *Tomolus*); eye adpressed closely to the head surface and with concave anterior and posterior eye margin; ocelli absent; antennal shield absent; pedicellus slightly to moderately curved; pedicellus ventrally inserted on scapus so that pedicellus and flagellomeres point posteriorly; pedicellus strongly curved; labrum completely sclerotized; ventral margin of second visible labial segment straight or concave. Thorax: posterolateral margin of pronotum surpassing or slightly surpassing medial pronotal margin; scutellum with well-developed medial process only; apex of short prosternal stridulatory process acute; tibiae lacking fossula spongiosa; tarsi three-segmented, hemelytron reaching or extending a little beyond abdominal apex. Abdomen: DAGs I–III ostioles present in adults and of similar sizes. *Female*. As in diagnosis.

Comments. Villiers (1943) erected the tribe as a member of the Tribelocephalinae and included all of the genera in our new

tribe Abelocephalini, as well as *Tomolus* and *Tribelocephala*. The tribe was once diagnosed by the absence of the proximal m-cu cross-vein in the hemelytra. *Acanthorhinocoris* was initially assigned to the Tribelocephalinae, but Rédei (2007) transferred the genus to the Opistoplatyini based on the presence of the proximal m-cu cross vein. Based on our results, we revise the Tribelocephalini and establish two subtribes: the Opistoplatyina and Tribelocephalina. Based on our diagnostic features and other morphological characters, we include *Acanthorhinocoris*, *Centrogastocoris*, *Distantus*, *Opistoplatys*, *Plectrophorocoris*, *Redeicephala, Tribelocephala* and *Tomolus*.

Opistoplatyina subtrib.n.

http://zoobank.org/urn:lsid:zoobank.org:act:1D091031-FA34-40D4-8E5B-9A364619B043
(Fig. 4J, P)

Type genus. Opistoplatys Westwood, 1834, 20: 447.

Diagnosis. Male. Diagnosed by the eyes reaching or nearly reaching the dorsal and ventral surfaces of the head (29–1, 30–1), antennal insertion laterally concealing suture between maxillary and mandibular plates (34–1), scapus without apical lobes, a prominent postscutum (84–1; Fig. 4J), and the proximal parts of M and Cu forming separate veins in the hemelytron (143–0; Fig. 4P). *Female.* As in male diagnosis.

Description. Male. As in diagnosis. *Female.* Similar to male.

Comments. This subtribe retains the same generic composition as the previously recognized Opistoplatyini: *Acanthorhinocoris*, *Centrogastocoris*, *Distantus*, *Opistoplatys*, *Plectrophorocoris* and *Redeicephala*.

Tribelocephalina subtrib.n.

http://zoobank.org/urn:lsid:zoobank.org:act:BEF5C321-3EDE-4922-B0A6-FC43C0075B8E
(Fig. 4C, O)

Type genus. Tribelocephala Stål, 1853, 10: 263.

Diagnosis. Male. Recognized by the antennal insertion ventral to the suture between the maxillary and mandibular plates (34–2; Fig. 4C), scapus with ventroanterior and ventroposterior apical lobes (36–1, 37–1; Fig. 4E), a reduced or absent postscutum (84–0), and the proximal parts of M and Cu forming a fused vein in the hemelytron (143–1; Fig. 4O). *Female*. Similar to male.

Description. Male. As in diagnosis. *Female*. Similar to male.

Comments. We include *Tribelocephala* and *Tomolus* in this subtribe based on the diagnosis.

Xenocaucini Maldonado

Type genus. Xenocaucus China & Usinger, 1959, 64: 43.

Diagnosis. Male. Recognized among Ectrichodiinae **sensu n.** by the reniform eyes adpressed close to the head (26–0) and a three-segmented distiflagellomere (43–2). We also recognize other diagnostic features that were recently described by Weirauch *et al.* (2016) for the only genus in this tribe, such as the long, slender scape that is ventrally excavated (surrounded by long fringes of setae), the two-segmented tarsi and a large, club-shaped Cu-Pcu cell in the hemelytra. *Female.* Apterous, eyes comprising two or three ommatidia, and tarsi one-segmented.

Redescription. Male. Vestiture: dense, consisting of long, slender setae on scapus, head laterally, lateral pronotal and scutellar margins, costal wing margin and lateral margin of dorsal laterotergites; bulbous trichomes present. Structure, head: with distinct lateral 'tuft', row of bulbous trichomes lateral to labium (forming a rostral groove); adpressed reniform eyes; scape slender, curved apically, with glabrous, excavated ventral surface bordered by posterolateral margin with row of long setae, dorsally with sparse short setae; pedicel shorter than scape, slender; flagellum short, very slender, subdivided into one basiflagellomere and three distiflagellomeres. Thorax: pronotum trapezoidal, anterior pronotal lobe much shorter than posterior pronotal lobe, metasternum with large bilobed process; legs slender; tarsi two-segmented; corium restricted to subcostal margin, with cell enclosed by Sc and proximal part of M + Cu; club-shaped Cu + Pcu cell large with narrow 'handle' basally; M + Cu cell large and trapezoid; claval furrow indistinct. Abdomen: DAGs II and III ostioles present in adults and of similar sizes. *Female*. Apterous, eyes reduced to a few ommatidia, pronotum subquadrate with anterior and posterior pronotal lobes not distinctly separated by a transverse suture, metasternum with or without bilobed process, legs typically stouter, and tarsi one-segmented.

Comments. This tribe only includes *Xenocaucus*, which was recently redescribed by Weirauch *et al*. (2016). Male diagnostic features are based on the only known male specimen of this tribe (*Xenocaucus ethiopiensis*) (Weirauch *et al*., 2016).

Supporting Information

Additional Supporting Information may be found in the online version of this article under the DOI reference: 10.1111/syen.12232

File S1. Twenty-eight female-based terminal taxa, with sources of male morphological data for 12 taxa indicated. I, digital images; T, taxonomic descriptions; M, direct examination of specimens at the Natural History Museum, London, U.K., and/or the American Museum of Natural History, New York, New York, U.S.A.

File S2. Morphological character matrix in nexus format for cladistic analysis.

File S3. Molecular character matrix in nexus format for cladistic analysis.

Figure S1. Molecular phylogenetic analyses of 59 taxa. Terminal taxon names are coloured by clades recovered in the combined morphological and molecular ML best tree in Fig. 3 for comparison. (A) Strict consensus tree from two parsimonious trees (length = 9181 steps; RI = 0.484; CI = 0.306). (B) ML best tree (final ln = −38481.3284) based on three partitions and models of sequence evolution: 16S, 28S D2, 28S, D3–D5 (GTR+Γ+I); 18S, COI codon positions 1 and 2, Wg (GTR+Γ+I); COI codon position 3 (HKY+Γ+I). (C) Bayesian MCMC majority-rule consensus tree based on the same three partitions and models of sequence evolution. Bootstrap values ≥50 are reported in A and B. Posterior probabilities ≥50 are reported in C. Grey labels above nodes or near higher-level taxon labels refer to clades discussed in the text.

Figure S2. Strict consensus tree from 269 parsimonious trees (length = 1203 steps; RI = 0.705; CI = 0.174) based on TNT analysis of 156 taxa (outgroups removed from figure) and morphological data. Terminal taxon names are coloured by clades recovered in the combined morphological and molecular ML best tree in Fig. 3 for comparison. Bootstrap values ≥50 are reported.

Figure S3. ML and Bayesian morphological phylogenetic analyses of 156 taxa (outgroups removed from figure). Terminal taxon names are coloured by clades recovered in the combined morphological and molecular ML best tree in Fig. 3 for comparison. (A) ML best tree (final ln = −5215.5335) based on Lewis (2001) Mkv model of morphological evolution. (B) Bayesian MCMC majority-rule consensus tree based on the same models of morphological evolution. Bootstrap values ≥50 are reported in (A). Posterior probabilities ≥50 are reported in (B). Grey label next to node in (A) refers to a clade discussed in the text.

Figure S4. Combined morphological parsimony phylogenetic analyses of 156 taxa (outgroups removed from figure) based on equal ('EW') and implied weights ($k = 3.000000$, 'IW3') TNT analyses. Terminal taxon names are coloured by clades recovered in the combined morphological and molecular ML best tree in Fig. 3 for comparison. Bootstrap values ≥50 are reported. (A) EW strict consensus tree from 664 parsimonious trees (length = 10 458 steps; RI = 0.527; CI = 0.288). (B) IW3 single most parsimonious tree (length = 753.08685 steps; RI = 0.519; CI = 0.285). Node labels in grey refer to clades discussed in the text.

Figure S5. Combined morphological parsimony phylogenetic analyses of 156 taxa (outgroups removed from figure) based on implied weights ($k = 4.266835$, 'IW4'; $k = 18.980060$, 'IW19') TNT analyses. Terminal taxon names are coloured by clades recovered in the combined morphological and molecular ML best tree in Fig. 3 for comparison. Bootstrap values ≥50 are reported. (A) IW4 single most parsimonious tree (length = 652.353 68 steps; RI = 0.520; CI = 0.285). (B) IW19 strict consensus tree from three parsimonious trees (length = 274.396 10 steps; RI = 0.526; CI = 0.288). Node labels in grey refer to clades discussed in the text.

Figure S6. Bayesian MCMC majority-rule consensus tree based on of 156 taxa (outgroups removed from figure) and a combined morphological and molecular dataset. Molecular data were divided into three partitions and models of sequence evolution: 16S, 28S D2, 28S, D3–D5 (GTR+Γ+I); 18S, COI codon positions 1 and 2, Wg (GTR+Γ+I); COI codon position 3 (HKY+Γ+I). Morphological data were analysed under Lewis (2001) Mkv model of morphological evolution. Terminal taxon names are coloured by clades recovered in the combined morphological and molecular ML best tree in Fig. 3 for comparison. Posterior probabilities ≥50 are reported. Node labels in grey refer to clades discussed in the text.

Figure S7. Parsimony ancestral sexual dimorphism reconstruction on the ML topology (Fig. 3) for Ectrichodiinae **sensu n.** (tree converted to cladogram for visual). Sexual dimorphism for terminal taxa coded as limited (black) or extreme (blue). Missing data (grey) for terminals is indicated.

Table S1. Morphological characters and character state coding.

Table S2. Molecular taxon sampling, USI and lab internal (RCW) codes, depositories, and GenBank accession numbers for sequenced specimens. Asterisks indicate sequences retrieved from GenBank.

Table S3. PCR protocols for each targeted gene region. Denaturation, annealing, and extension were conducted for 35 cycles for all gene regions sampled.

Table S4. BAYESTRAITS MultiState ML and MCMC ASR output for sexual dimorphism on ML phylogram and ultrametric trees. The grey panel lists internal node IDs and subtending terminal taxa. The blue panel are results from ML ASR. The yellow panel are results from MCMC ASR. Ultra 0, ultrametric tree generated with penalty set to 0; Ultra 10, ultrametric tree generated with penalty set to 10; Ultra 10 000, ultrametric tree generated with penalty set to 10 000. Accessible through the following Figshare DOI: 10.6084/m9.figshare.4702852.

Acknowledgements

We would like to extend our appreciation to those who donated or loaned specimens for this project: Jean-Michel Berenger, Dominik Chłond, Eliane de Coninck, Jason Cryan, David Grimaldi, Eric Guilbert, Tom Henry, Michael Ivie, John Longino, Rudolf Meier, Joshua Oyelade, Norm Penny, Dávid Rédei, Ruth Salas, Toby Schuh, Michael Sharkey, David Wagner, Mick Webb, and the students and instructors of the 2010 Organization for Tropical Studies field course in Costa Rica. Bernard Dupont, Eduard Jendek, Steve Marshall, Bonnie Ott, and Melvyn Yeo contributed photographs of Ectrichodiinae species for this manuscript. We also thank Mark Springer, Bradley Mullens, and current and former members of the John Hearty, Christiane Weirauch and Christine Miller laboratories for valuable feedback on various aspects of the project and the manuscript. This work was funded by the National Science Foundation (NSF) PEET DEB 093333853 grant (awarded to CW) and the Entomological Society of America Systematic, Evolution, and Biodiversity Travel Award; Earle C. Anthony Graduate Student Travel Award; Graduate Dean's Dissertation Research Grant; and the University of California – Riverside Graduate Division Dissertation Year Program Award (awarded to MF). Some specimens loaned for this research were acquired under NSF DEB 0542864 (awarded to Michael Sharkey and Brian Brown), NSF BSI 0072713 (awarded to Brian Fisher and Charles Griswold) and NSF DEB 1354739 (awarded to John Longino).

References

Allen, C.E., Zwaan, B.J. & Brakefield, P.M. (2011) Evolution of sexual dimorphism in the Lepidoptera. *Annual Review of Entomology*, **56**, 445–464.

Andersen, N.M. (1997) A phylogenetic analysis of the evolution of sexual dimorphism and mating systems in water striders (Hemiptera: Gerridae). *Biological Journal of the Linnean Society*, **61**, 345–368.

Baker, R.H. & Wilkinson, G.S. (2001) Phylogenetic analysis of sexual dimorphism and eye-span alllometry in stalk-eyed flies (Diopsidae). *Evolution*, **55**, 1373–1385.

Binford, G.J., Gillespie, R.G. & Maddison, W.P. (2016) Sexual dimorphism in venom chemistry in *Tetragnatha* spiders is not easily explained by adult niche differences. *Toxicon*, **114**, 45–52.

Bocak, L., Bocakova, M., Hunt, T. & Vogler, A.P. (2008) Multiple ancient origins of neoteny in Lycidae (Coleoptera): consequences for ecology and macroevolution. *Proceedings of the Royal Society of London Series B*, **275**, 2015–2023.

Bocakova, M., Bocak, L., Hunt, T., Teraväinen, M. & Vogler, A.P. (2007) Molecular phylogenetics of Elateriformia (Coleoptera): evolution of bioluminescence and neoteny. *Cladistics*, **23**, 477–496.

Bromham, L., Woolfit, M., Lee, M.S.Y. & Rambaut, A. (2002) Testing the relationship between morphological and molecular rates of change along phylogenies. *Evolution*, **56**, 1921–1930.

Cooper, I.A., Brown, J.M. & Getty, T. (2016) A role for ecology in the evolution of colour variation and sexual dimorphism in Hawaiian damselflies. *Journal of Evolutionary Biology*, **29**, 418–427.

Cryan, J.R., Liebherr, J.K., Fetzner, J.W. Jr. & Whiting, M.F. (2001) Evaluation of relationships within the endemic Hawaiian Platynini (Coleoptera: Carabidae) based on molecular and morphological evidence. *Molecular Phylogenetics and Evolution*, **21**, 72–85.

Cusimano, N. & Renner, S.S. (2014) Ultrametric trees or phylograms for ancestral state reconstruction: does it matter? *Taxon*, **63**, 721–726.

Dallwitz, M.J. (1980) A general system for coding taxonomic descriptions. *Taxon*, **29**, 41–46.

Dallwitz, M.J., Paine, T.A. & Zurcher, E.J. (1999) *User's Guide to the DELTA Editor* [WWW document]. URL http://delta-intkey.com [accessed on 2 February 2014].

Damgaard, J., Andersen, N.M., Cheng, L. & Sperling, F.A.H. (2000) Phylogeny of sea skaters, *Halobates* Eschscholtz (Hemiptera, Gerridae), based on mtDNA sequence and morphology. *Zoological Journal of the Linnean Society*, **130**, 511–526.

Darwin, C. (1859) *The Origin of Species*. John Murray, London.

Darwin, C. (1871) *The Descent of Man and Selection in Relation to Sex*. Princeton University Press, Princeton, New Jersey.

Davranoglou, L.R. (2016) *Redeicephala taylori*, a new genus and species of Reduviidae from New Guinea, with notes on a few morphological features of the Tribelocephalinae (Hemiptera: Heteroptera). *Acta Entomologica Musei Nationalis Pragae*, **56**, 39–50.

Denno, R.F., Olmstead, K.L. & McCloud, E.S. (1989) Reproductive cost of flight capability: a comparison of life history traits in wing dimorphic planthoppers. *Ecological Entomology*, **14**, 31–44.

Disney, R.H.L. (1996) A new genus of scuttle fly (Diptera; Phoridae) whose legless, wingless, females mimic ant larvae (Hymenoptera; Formicidae). *Sociobiology*, **27**, 95–118.

Dougherty, V. (1995) A review of the New World Ectrichodiinae genera (Hemiptera: Reduviidae). *Transactions of the American Entomological Society*, **121**, 173–225.

Emlen, D.J., Hunt, J. & Simmons, L.W. (2005) Evolution of sexual dimorphism and male dimorphism in the expression of beetle horns: phylogenetic evidence for modularity, evolutionary lability, and constraint. *The American Naturalist*, **166**, S42–S68.

Forero, D. & Weirauch, C. (2012) Comparative genitalic morphology in the New World resin bugs Apiomerini (Hemiptera, Heteroptera, Reduviidae, Harpactorinae). *Deutsche Entomologische Zeitschrift*, **59**, 5–41.

Forero, D., Berniker, L. & Weirauch, C. (2013) Phylogeny and character evolution in the bee-assassins (Insecta, Heteroptera: Reduviidae). *Molecular Phylogenetics and Evolution*, **66**, 283–302.

Forthman, M. & Weirauch, C. (2012) Toxic associations: a review of the predatory behaviors of millipede assassin bugs (Hemiptera: Reduviidae: Ectrichodiinae). *European Journal of Entomology*, **109**, 147–153.

Forthman, M. & Weirauch, C. (2016) Phylogenetics and biogeography of the endemic Madagascan millipede assassin bugs (Heteroptera: Reduviidae: Ectrichodiinae). *Molecular Phylogenetics and Evolution*, **100**, 219–233.

Forthman, M., Chłond, D. & Weirauch, C. (2016) Taxonomic monograph of the endemic millipede assassin bug fauna of Madagascar (Hemiptera: Reduviidae: Ectrichodiinae). *Bulletin of the American Museum of Natural History*, **400**, 1–152.

Goloboff, P.A. (1993) Estimating character weights during tree search. *Cladistics*, **9**, 83–91.

Goloboff, P.A., Farris, J.S. & Nixon, K.C. (2008) TNT, a free program for phylogenetic analysis. *Cladistics*, **24**, 774–786.

Gullan, P.J. & Kosztarab, M. (1997) Adaptations in scale insects. *Annual Review of Entomology*, **42**, 23–50.

Hedrick, A.V. & Temeles, E.J. (1989) The evolution of sexual dimorphism in animals: hypotheses and tests. *Trends in Ecology & Evolution*, **4**, 136–138.

Hill, L. (2014) Revision of *Silhouettanus* with description of nine new species (Hemiptera: Heteroptera: Schizopteridae). *Zootaxa*, **3815**, 353–385.

Hwang, W.S. & Weirauch, C. (2012) Evolutionary history of assassin bugs (Insecta: Hemiptera: Reduviidae): insights from divergence dating and ancestral state reconstruction. *PLoS ONE*, **7**, e45523.

Ishikawa, T., Cai, W. & Tomokuni, M. (2015) The assassin bug subfamily Tribelocephalinae (Hemiptera: Heteroptera: Reduviidae) from Japan, with descriptions of eight new species in the genera *Opistoplatys* and *Abelocephala*. *Zootaxa*, **3936**, 151–180.

Kathirithamby, J. (1989) Review of the order Strepsiptera. *Systematic Entomology*, **14**, 41–92.

Katoh, K. & Standley, D.M. (2013) MAFFT multiple sequence alignment software version 7: improvements in performance and usability. *Molecular Biology and Evolution*, **30**, 772–780.

Kundrata, R. & Bocak, L. (2011) The phylogeny and limits of Elateridae (Insecta: Coleoptera): is there a common tendency of click beetles to soft-bodiedness and neoteny? *Zoologica Scripta*, **40**, 364–378.

Lande, R. (1980) Sexual dimorphism, sexual selection, and adaptation in polygenic characters. *Evolution*, **34**, 292–305.

Lanfear, R., Calcott, B., Ho, S.Y.W. & Guindon, S. (2012) PartitionFinder: combined selection of partitioning schemes and substitution models for phylogenetic analyses. *Molecular Biology and Evolution*, **29**, 1695–1701.

Lewis, P.O. (2001) A likelihood approach to estimating phylogeny from discrete morphological character data. *Systematic Biology*, **50**, 913–925.

Litsios, G. & Salamin, N. (2012) Effects of phylogenetic signal on ancestral state reconstruction. *Systematic Biology*, **61**, 533–538.

Maddison, W.P. & Maddison, D.R. (2015) *Mesquite: A Modular System for Evolutionary Analysis*. Version 3.02. [WWW document]. URL http;//mesquiteproject.org [accessed on 14 January 2015].

Maldonado, J. (1990) Systematic catalogue of the Reduviidae of the world (Insecta: Heteroptera). *Caribbean Journal of Science*, Special Edition, pp. 1–694.

Maldonado, J. (1996) New taxa and key to the tribes and genera in Tribelocephalinae Stål 1866 (Heteroptera: Reduviidae). *Proceedings of the Entomological Society of Washington*, **98**, 138–144.

Mirande, J.M. (2009) Weighted parsimony phylogeny of the family Characidae (Teleostei: Characiformes). *Cladistics*, **25**, 574–613.

Oakley, T.H. (2005) Myodocopa (Crustacea: Ostracoda) as models for evolutionary studies of light and vision: multiple origins of bioluminescence and extreme sexual dimorphism. *Hydrobiologia*, **538**, 179–192.

Omland, K.E. (1997) Correlated rates of molecular and morphological evolution. *Evolution*, **51**, 1381–1393.

Pagel, M., Meade, A. & Barker, D. (2004) Bayesian estimation of ancestral character states on phylogenies. *Systematic Biology*, **53**, 673–684.

Punzalan, D. & Rowe, L. (2016) Concordance between stabilizing sexual selection, intraspecific variation, and interspecific divergence in *Phymata*. *Ecology and Evolution*. **6**, 7997–8009.

Rambaut, A. & Drummond, A.J. (2015) *TreeAnnotater*. Version 2.3.2. [WWW document]. URL http://beast2.org/ [accessed on 6 June 2014].

Rambaut, A., Suchard, M.A., Xie, W. & Drummond, A.J. (2014) *Tracer*. Version 1.61. [WWW document]. URL http://tree.bio.ed.ac.uk/software/tracer/ [accessed on 6 June 2014].

Rédei, D. (2007) A new genus of tribelocephaline assassin bugs from Borneo (Hemiptera: Heteroptera: Reduviidae). *Zootaxa*, **1465**, 47–53.

Rédei, D. & Tsai, J.-F. (2012) The assassin bug genus *Haematoloecha* in Taiwan, with notes on species occurring in neighbouring areas (Hemiptera: Heteroptera: Reduviidae: Ectrichodiinae). *Zootaxa*, **3332**, 1–26.

Rédei, D., Ren, S. & Bu, W. (2012) A new synonymy in the genus *Rhysostethus* (Hemiptera: Heteroptera: Reduviidae). *Acta Entomologica Musei Nationalis Pragae*, **52**, 341–348.

Reemer, M. & Ståhls, G. (2012) *Unravelling a hotchpotch: phylogeny and classification of the microdontinae (Diptera: Syrphidae)*. PhD Dissertation, Leiden University, Leiden.

Roff, D.A. (1986) The evolution of wing dimorphism in Insecta. *Evolution*, **40**, 1009–1020.

Roff, D.A. (1990) The evolution of flightlessness in Insecta. *Ecological Monographs*, **60**, 389–421.

Roff, D.A. & Fairbairn, D.J. (1991) Wing dimorphisms and the evolution of migratory polymorphisms among the Insecta. *American Zoologist*, **31**, 243–251.

Ronquist, F., Teslenko, M., van der Mark, P. *et al.* (2012) MrBayes 3.2: efficient Bayesian phylogenetic inference and model choice across a large model space. *Systematic Biology*, **61**, 539–542.

Sanderson, M.J. (2002) Estimating absolute rates of molecular evolution and divergence times: a penalized likelihood approach. *Molecular Biology and Evolution*, **19**, 101–109.

Sanderson, M.J. (2003) r8s: inferring absolute rates of molecular evolution and divergence times in the absence of a molecular clock. *Bioinformatics*, **19**, 301–302.

Shine, R. (1989) Ecological causes for the evolution of sexual dimorphism: a review of the evidence. *The Quarterly Review of Biology*, **64**, 419–461.

Simon, C., Frati, F., Beckenbach, A., Crespi, B., Liu, H. & Flook, P. (1994) Evolution, weighting, and phylogenetic utility of mitochondrial gene sequences and a compilation of conserved polymerase chain reaction primers. *Annals of the Entomological Society of America*, **87**, 651–701.

Slater, J.A. (1977) The incidence and evolutionary significance of wing polymorphism in lygaeid bugs with particular reference to those of South Africa. *Biotropica*, **9**, 217–229.

Smith, S.A. & Donoghue, M.J. (2008) Rates of molecular evolution are linked to life history in flowering plants. *Science*, **322**, 86–89.

Stål, C. (1865) Hemiptera Africana. *Öfversigt af Kongliga Vetenskaps-Akademiens Förhandlingar*, **3**, 1–200.

Teder, T. & Tammaru, T. (2005) Sexual size dimorphism within species increases with body size in insects. *Oikos*, **108**, 321–334.

Urban, J.M. & Cryan, J.R. (2007) Evolution of the planthoppers (Insecta: Hemiptera: Fulgoroidea). *Molecular Phylogenetics and Evolution*, **42**, 556–572.

Vaidya, G., Lohman, D.J. & Meier, R. (2011) SequenceMatrix: concatenation software for the fast assembly of multi-gene datasets with character set and codon information. *Cladistics*, **27**, 171–180.

Villiers, A. (1943) Morphologie et systématique des Tribelocephalitae africains. *Revue Française d'Entomologie*, **10**, 1–28.

Wagner, D.L. & Liebherr, J.K. (1992) Flightlessness in insects. *Trends in Ecology and Evolution*, **7**, 216–220.

Weirauch, C. (2006) Dorsal abdominal glands in adult Reduviidae (Heteroptera, Cimicomorpha). *Deutsche Entomologische Zeitschrift*, **53**, 91–102.

Weirauch, C. (2008) Cladistic analysis of Reduviidae (Heteroptera: Cimicomorpha) based on morphological characters. *Systematic Entomology*, **33**, 229–274.

Weirauch, C. (2010) *Tribelocodia ashei*, new genus and new species of Reduviidae (Insecta: Hemiptera), has implications on character evolution in Ectrichodiinae and Tribelocephalinae. *Insect Systematics and Evolution*, **41**, 103–122.

Weirauch, C. & Munro, J.B. (2009) Molecular phylogeny of the assassin bugs (Hemiptera: Reduviidae), based on mitochondrial and nuclear ribosomal genes. *Molecular Phylogenetics and Evolution*, **53**, 287–299.

Weirauch, C., Forthman, M., Grebennikov, V. & Baňař, P. (2016) From Eastern Arc Mountains to extreme sexual dimorphism: systematics of the enigmatic assassin bug genus *Xenocaucus* (Hemiptera: Reduviidae: Tribelocephalinae). *Organisms Diversity & Evolution*. https://doi.org/10.1007/s13127-016-0314-2.

Whiting, M.F., Bradler, S. & Maxwell, T. (2003) Loss and recovery of wings in stick insects. *Nature*, **421**, 264–267.

Zhang, J., Gordon, E., Forthman, M. *et al.* (2016) Evolution of the assassin's arms: insights from a phylogeny of combined transcriptomic and ribosomal DNA data (Heteroptera: Reduvioidea). *Scientific Reports*, **6**, 22177.

Zwickl, D.J. (2006) *Genetic algorithm approaches for the phylogenetic analysis of large biological sequence datasets under the maximum likelihood criterion*. PhD Dissertation, University of Texas, Austin.

Zwickl, D.J. (2008) *GARLI Manual*. [WWW document]. URL : https://code.google.com/archive/p/garli/downloads [accessed on 14 January 2015].

Accepted 1 March 2017